Combined analysis of $B_c \to D_s^{(*)}\mu^+\mu^-$ and $B_c \to D_s^{(*)}\nu\bar{\nu}$ decays within Z' and leptoquark new physics models

Manas K. Mohapatra,[1,*] N. Rajeev,[2,†] and Rupak Dutta[2,‡]

[1]*Department of Physics, Indian Institute of Technology Hyderabad, Kandi - 502285, India*
[2]*National Institute of Technology Silchar, Silchar 788010, India*

(Received 29 September 2021; accepted 20 May 2022; published 16 June 2022)

We investigate the exclusive rare semileptonic decays $B_c \to D_s^{(*)}(\ell\ell, \nu\bar{\nu})$ induced by neutral current transition $b \to s(\ell\ell, \nu\bar{\nu})$ in the presence of nonuniversal Z', scalar and vector leptoquark new physics models. We constrain the new physics parameter space by using the latest experimental measurements of $R_{K^{(*)}}$, P_5', $\mathcal{B}(B_s \to \phi\mu^+\mu^-)$ and $\mathcal{B}(B_s \to \mu^+\mu^-)$. Throughout the analysis, we choose to work with the particular new physics scenario $C_9^{\mu\mu}(NP) = -C_{10}^{\mu\mu}(NP)$ where both Z', $S_{1/3}^3$, and $U_{-2/3}^3$ leptoquarks satisfy the condition. Using these new coupling parameters, we scrutinize the several physical observables such as differential branching fraction, the forward backward asymmetry, the lepton polarization asymmetry, the angular observable P_5', and the lepton flavor universal sensitive observables, including the ratio of branching ratio $R_{D_s^{(*)}}$ and the few Q parameters in the $B_c \to D_s^{(*)}\mu^+\mu^-$ and $B_c \to D_s^{(*)}\nu\bar{\nu}$ decay processes.

DOI: 10.1103/PhysRevD.105.115022

I. INTRODUCTION

The hint of new physics (NP) in the form of new interactions, which demands an extension of the standard model (SM) of particle physics are witnessed not only in the flavor changing neutral current decays of rare beauty particles of the form $b \to s\ell^+\ell^-$ but also in the flavor changing charged current decays proceeding via $b \to c\ell\nu$ quark level transitions. The rare weak decays of several composite beauty mesons such as B_d, B_s, and B_c, which are forbidden at the tree level in SM, appear to follow loop or box level diagrams. Theoretically, the radiative and semileptonic decays of $B \to K^{(*)}$ and $B_s \to \phi$ processes have received greater attention and are studied extensively both within the SM and beyond. The sensitivity of new physics possibilities in these decays requires very good knowledge of the hadronic form factors, more specifically for $B \to V$ transitions. It requires information from both the light cone sum rule (LCSR) and lattice QCD (LQCD) methods to compute the form factors, respectively, at low and high q^2 regions, which eventually confine the whole kinematic region [1]. Currently, we do have the very precise calculations of the form factors that have very accurate SM predictions of the differential branching fractions and various angular observables in $b \to s\ell^+\ell^-$ decays. Similarly, the family of neutral decays proceeding via $b \to s\nu\bar{\nu}$ transitions equally provide the interesting opportunity in probing new physics signatures to that of $b \to s\ell^+\ell^-$ transitions. However, so far no experiments have directly addressed any anomalies except the upper bounds of the branching fractions of $B \to K^{(*)}\nu\bar{\nu}$ decay processes. In principle, under the $SU(2)_L$ gauge symmetry, both the charged leptons and neutral leptons are treated equally, and hence, one can extract a close relation between both $b \to s\ell^+\ell^-$ and $b \to s\nu\bar{\nu}$ decays in beyond the SM scenarios. In addition, the decays with $\nu\bar{\nu}$ final state are well motivated for several interesting features since these decays are considered to be theoretically cleaner as they do not suffer from hadronic uncertainties beyond the form factors such as the nonfactorizable corrections and photonic penguin contributions.

Experimentally, several measurements in $b \to s\ell^+\ell^-$ transitions, such as $R_{K^*} = \mathcal{B}(B \to K^*\mu^+\mu^-)/\mathcal{B}(B \to K^*e^+e^-)$ from LHCb [2,3] and Belle [4] at $q^2 \in [0.045, 1.1]$ and $q^2 \in [1.1, 6.0]$ show 2.1–2.4σ deviation from the SM expectations [5,6]. Similarly, the angular observable P_5' in $B \to K^*\mu^+\mu^-$ from in the bins $q^2 \in [4.0, 6.0]$, $[4.3, 6.0]$ and $[4.0, 8.0]$ from ATLAS [7], LHCb [8,9], CMS [10], Belle [11], respectively, deviate at 3.3σ, 1σ, and 2.1σ from the SM expectations [12–14]. The recent updates in the measurements of $R_K = \mathcal{B}(B \to K\mu^+\mu^-)/\mathcal{B}(B \to Ke^+e^-)$ [15,16] in $q^2 \in [1.0, 6.0]$ and the branching fraction of $\mathcal{B}(B_s \to \phi\mu^+\mu^-)$ [17–19] in $q^2 \in [1.1, 6.0]$ region from LHCb still indicate 3.1σ in R_K

*manasmohapatra12@gmail.com
†rajeev_rs@phy.nits.ac.in
‡rupak@phy.nits.ac.in

[5,6] and 3.6σ in $\mathcal{B}(B_s \to \phi\mu^+\mu^-)$ [1,20] from the SM expectations. Similarly, the measurements pertaining to $b \to s\nu\bar{\nu}$ transitions, the upper bound measured by the Belle Collaboration in the branching fraction of $B \to K^{(*)}\nu\bar{\nu}$ decays are $\mathcal{B}(B \to K\nu\bar{\nu}) < 1.6 \times 10^{-5}$ and $\mathcal{B}(B \to K^*\nu\bar{\nu}) < 2.7 \times 10^{-5}$ [21], respectively. There also exist the *BABAR* measurement on $\mathcal{B}(B \to K^*\nu\bar{\nu}) < 4 \times 10^{-5}$ [22]. Very recently, the Belle II updated the upper bound of $\mathcal{B}(B \to K\nu\bar{\nu}) < 4.1 \times 10^{-5}$ in 2021 [23].

There exist several other decay channels similar to the $B \to K^{(*)}$ and $B_s \to \phi$ undergoing $b \to s\ell^+\ell^-$ quark level transitions [23–39]. If any new physics present in $B \to K^{(*)}$ and $B_s \to \phi$ decays can in principle be reflected in several other decays as well. In that sense, we choose to study the explicit rare decays $B_c \to D_s^{(*)}\mu^+\mu^-$ and $B_c \to D_s^{(*)}\nu\bar{\nu}$, which undergo similar $b \to s$ neutral transition. The particular decay modes $B_c \to D_s^{(*)}\mu^+\mu^-$ have been studied previously in SM using various form factors that include relativistic quark model (RQM) [40], the light front and constituent quark model [41,42], the three point QCD sum rules approach [43], the covariant quark model [44], and very recently, using the lattice QCD form factors only for $B_c \to D_s$ transitions [45]. In addition, as far as beyond SM analysis are concerned, these decays have also been analyzed within model independent and dependent new physics as well. The model independent study within the effective field theory approach was done in Ref. [46] under various 1D and 2D NP scenarios. In Ref. [47], the decay mode was studied within a nonuniversal Z' model with the NP contribution coming from only the right-handed currents. Similarly, the contribution of Z' was analyzed by considering the UTfit inputs of left-handed coupling of Z' boson and the different values of new weak phase angle in the Ref. [48]. Similarly, the SM results pertaining to the $B_c \to D_s^{(*)}\nu\bar{\nu}$ decays have been addressed in Refs. [40,42,49].

Even from the experimental point of view after the discovery of B_c meson at CDF via $B_c \to J/\Psi\ell\nu$ [50], the study of B_c decays were found to be very interesting. Unlike the weak decays of other B mesons, the B_c mesons are interesting as it is composed of both heavy b and c quarks that allows a broader kinematic range, which eventually involve large number of decays. In addition, the upcoming LHC run can produce around 10^8–10^{10} B_c mesons [51–55], which offer very rich laboratory for the associated B_c weak decays. At LHC with a luminosity 10^{34} cm^{-2} s^{-1}, one could expect around 2×10^{10} B_c events per year [56,57]. Hence, exploring the new physics in $B_c \to D_s^{(*)}\mu^+\mu^-$ decays are experimentally well motivated at the LHCb experiments.

For the experimental scope of the $B_c \to D_s^{(*)}\nu\bar{\nu}$ channels concerns, as we know, they are experimentally challenging because of the dineutrinos in the final state, which leave no information in the detector. However, recently, Belle II at SuperKEK uses a novel and independent inclusive tagging approach and measures the upper limit of the branching fraction of $B \to K\nu\bar{\nu}$ decays [58]. This novel method has benefited with larger signal efficiency of about 4%, at the cost of higher background level [58]. Since Belle and Belle II mainly work at $\Upsilon(4S)$ and $\Upsilon(5S)$ resonances, no B_c mesons are produced. Hence, study of $B_c \to D_s^{(*)}\nu\bar{\nu}$ channels would be difficult at the Belle II experiment. Moreover, as there are more number of B_c mesons produced at LHC, it can, in principle, be feasible to predict an upper limit of the branching fraction of $B_c \to D_s^{(*)}\nu\bar{\nu}$ decays in their future prospects.

In this context, we study the implication of the latest $b \to s\ell^+\ell^-$ data on the $B_c \to D_s^{(*)}\mu^+\mu^-$ and $B_c \to D_s^{(*)}\nu\bar{\nu}$ decay processes under the model dependent analysis. We choose in particular, the specific models such as Z' and the various scalar and vector leptoquarks (LQs), which satisfy $C_9^{\mu\mu}(NP) = -C_{10}^{\mu\mu}(NP)$ new physics scenario. Among various LQs, we opt for the specific LQs in such a way that they should have combined NP effects in the form of $C_9^{\mu\mu}(NP) = -C_{10}^{\mu\mu}(NP)$ both in $b \to s\ell^+\ell^-$ and $b \to s\nu\bar{\nu}$ decays. Hence, the main aim of this work is to extract the common new physics that appear simultaneously in $b \to s\ell^+\ell^-$ and $b \to s\nu\bar{\nu}$ decays.

The layout of the present paper is as follows. In Sec. II, we add a theoretical framework that includes a brief discussion of effective Hamiltonian for $b \to s\ell^+\ell^-$ and $b \to s\nu\bar{\nu}$ parton level transition. In addition to this, we also present the differential decay distributions and other q^2 dependent observables of $B_c \to D_s^{(*)}\mu^+\mu^-$ and $B_c \to D_s^{(*)}\nu\bar{\nu}$ processes. In the context of new physics, we deal with the contributions arising due to the exchange of LQ and Z' particles in Sec. III. In Sec. IV, we report and discuss our numerical analysis in the SM and in the presence of NP contributions. Finally, we end with our conclusion in Sec. V.

II. THEORETICAL FRAMEWORK

A. Effective Hamiltonian

The effective Hamiltonian responsible for $b \to s\ell\ell$ parton level transition in the presence of NP vector operator can be represented as [59]

$$\begin{aligned}\mathcal{H}_{\text{eff}} = -\frac{\alpha G_F}{\sqrt{2}\pi} V_{tb}V_{ts}^* \Big[& 2\frac{C_7^{\text{eff}}}{q^2}[\bar{s}\sigma^{\mu\nu}q_\nu(m_s P_L + m_b P_R)b](\bar{\ell}\gamma_\mu\ell) \\ & + C_9^{\text{eff}}(\bar{s}\gamma^\mu P_L b)(\bar{\ell}\gamma_\mu\ell) + C_{10}(\bar{s}\gamma^\mu P_L b)(\bar{\ell}\gamma_\mu\gamma_5\ell) \\ & + C_9^{\ell\ell}(\text{NP})(\bar{\text{s}}\gamma^\mu \text{P}_\text{L}\text{b})(\bar{\ell}\gamma_\mu\ell) \\ & + C_{10}^{\ell\ell}(\text{NP})\bar{\text{s}}\gamma^\mu \text{P}_\text{L}\text{b}\bar{\ell}\gamma_\mu\gamma_5\ell \Big], \end{aligned} \tag{1}$$

where G_F is the Fermi coupling constant, α is the fine structure constant, V_{ij} is the CKM matrix element, and $C_7^{\text{eff}}, C_9^{\text{eff}}$, and C_{10} are the relevant Wilson coefficients

(WC) evaluated at $\mu = m_b^{\rm pole}$ scale [59]. The Wilson coefficients $C_9^{\ell\ell}(\mathrm{NP})$ and $C_{10}^{\ell\ell}(\mathrm{NP})$ are the effective coupling constants associated with the corresponding NP operators. The effective Hamiltonian describing $b \to s\nu\bar{\nu}$ decay processes is given by [60]

$$\mathcal{H}_{\rm eff}^{\nu\bar{\nu}} = \frac{G_F \alpha}{2\sqrt{2}\pi} V_{tb} V_{ts}^* C_L^{\nu\nu} \mathcal{O}_L^{\nu\nu}. \tag{2}$$

Here, the effective four fermion operator $\mathcal{O}_L^{\nu\nu} = (\bar{s}\gamma_\mu P_L b)(\bar{\nu}\gamma^\mu(1-\gamma_5)\nu)$ and the associated coupling strength $C_L^{\nu\nu} = X(x_t)/s_W^2$, which includes the Inami—Lim function $X(x_t)$ given in Ref. [61]. In principle, several Lorentz structures in the form of chiral operators can be possible in the NP scenario, such as vector, axial vector, scalar, pseudoscalar, and tensor. However, among all the operators scalar, pseudoscalar, and tensor are severely constrained by $B_s \to \mu\mu$ and $b \to s\gamma$ measurements [62]. Therefore, we consider the vector and axial vector contributions only. In our analysis, among possible NP operators we consider only the left chiral $\mathcal{O}_9^{\ell\ell}(\mathrm{NP})$ and $\mathcal{O}_{10}^{\ell\ell}(\mathrm{NP})$ contributions and the associated Wilson coefficients are assumed to be real. The effective Wilson coefficients $C_7^{\rm eff}$ and $C_9^{\rm eff}$ are defined as [63]

$$\begin{aligned} C_7^{\rm eff} &= C_7 - \frac{C_5}{3} - C_6 \\ C_9^{\rm eff} &= C_9(\mu) + h(\hat{m}_c, \hat{s}) C_0 \\ &\quad - \frac{1}{2} h(1, \hat{s})(4C_3 + 4C_4 + 3C_5 + C_6) \\ &\quad - \frac{1}{2} h(0, \hat{s})(C_3 + 3C_4) \\ &\quad + \frac{2}{9}(3C_3 + C_4 + 3C_5 + C_6), \end{aligned} \tag{3}$$

where $\hat{s} = q^2/m_b^2$, $\hat{m}_c = m_c/m_b$, and $C_0 = 3C_1 + C_2 + 3C_3 + C_4 + 3C_5 + C_6$.

$$\begin{aligned} h(z, \hat{s}) &= -\frac{8}{9}\ln\frac{m_b}{\mu} - \frac{8}{9}\ln z + \frac{8}{27} + \frac{4}{9}x - \frac{2}{9}(2+x)|1-x|^{1/2} \\ &\quad \times \begin{cases} \ln\left|\frac{\sqrt{1-x}+1}{\sqrt{1-x}-1}\right| - i\pi, & \text{for } x \equiv \frac{4z^2}{\hat{s}} < 1 \\ 2\arctan\frac{1}{\sqrt{x-1}}, & \text{for } x \equiv \frac{4z^2}{\hat{s}} > 1 \end{cases} \end{aligned} \tag{4}$$

and

$$h(0, \hat{s}) = -\frac{8}{9}\ln\frac{m_b}{\mu} - \frac{4}{9}\ln\hat{s} + \frac{8}{27} + \frac{4}{9}i\pi. \tag{5}$$

Here, we have included the short distance perturbative contributions to $C_9^{\rm eff}$. The measurements of the $B \to (K^{(*)}, \phi)\ell\ell$ processes induced by $b \to s\ell\ell$ quark level transition, in principle, include the available vector resonances. These regions arise in the dimuon invariant mass resonance $m_{\mu\mu}$ around $\phi(1020), J/\psi(3096)$, and $\psi_{2S}(3686)$ along with broad charmonium states $\psi(3770), \psi(4040), \psi(4160)$, and $\psi(4415)$. The amplitudes in these regions though are dominated but have a large theoretical uncertainty. However, this is performed with a model describing these vector resonances as a sum of the relativistic Breit-Wigner amplitudes. The explicit expressions of the $c\bar{c}$ resonance part reads

$$\mathcal{Y}_{\rm BW}(q^2) = \frac{3\pi}{\alpha^2} \sum_{V_i = J/\psi, \psi'} \frac{\Gamma(V_i \to \ell^+\ell^-) M_{V_i}}{M_{V_i}^2 - q^2 - i M_{V_i}\Gamma_{V_i}}, \tag{6}$$

where $M_{V_i}(J/\psi, \psi')$ is the mass of the vector resonance and Γ_{V_i} is the total decay width of the vector mesons. Moreover, in our study, we have taken care by avoiding all the $c\bar{c}$ resonances appearing at respective q^2 regions. Hence, our all predictions concerned to $b \to s\mu^+\mu^-$ decay observables are done in the q^2 regions [0.1–0.98] and [1.1–6] GeV^2. On the other hand, the case with $b \to s\nu\bar{\nu}$ quark level transitions are quite different. In principle, $b \to s\nu\bar{\nu}$ decays are free from various hadronic uncertainties beyond the form factors, such as the nonfactorizable corrections and photonic penguin contributions. In particular, the vector charmonium states including $\phi(1020)$, $J/\psi(3096)$, and $\psi_{2S}(3686)$ etc. do not contribute to any dineutrino states in the concerned decays of $b \to s\nu\bar{\nu}$ channels. Hence, one can access the whole q^2 region in the prediction of various observables in $B_c \to D_s^{(*)}\nu\bar{\nu}$ decays. Hence, the $b \to s\nu\bar{\nu}$ decay channels are treated as theoretically cleaner than the $b \to s\ell\ell$ decay processes. Apart from this, additionally we do not even include any nonlocal effects in our analysis, which are important below the charmonium contributions that have been studied in detail in Refs. [64–67]. In principle, these hadronic non local effects are generally neglected in the study of the lepton flavor universality violation (LFUV) in various $b \to s\ell\ell$ decays. In addition, the factorizable effects arising due to the spectator scattering may not affect severely to the LFU ratios, and hence, these effects are neglected in our present analysis [68,69].

B. Differential decay distribution and q^2 observables in $B_c \to D_s^{(*)}\mu^+\mu^-$

In analogy with $B \to K\ell^+\ell^-$ decay mode, it is useful to note that the rare semileptonic $B_c \to D_s\ell^+\ell^-$ process is also mediated through $b \to s\ell^+\ell^-$ transition in the parton level. In the standard model, we present the formula of q^2 dependent differential branching ratio which is given as follows [70]:

$$\frac{d\mathrm{BR}}{dq^2} = \frac{\tau_{B_c}}{\hbar}\left(2a_\ell + \frac{2}{3}c_\ell\right), \tag{7}$$

where the parameters a_ℓ and c_ℓ are given by

$$a_\ell = \frac{G_F^2\alpha_{\rm EW}^2|V_{tb}V_{ts}^*|^2}{2^9\pi^5 m_{B_c}^3}\beta_\ell\sqrt{\lambda}\Big[q^2|F_P|^2 + \frac{\lambda}{4}(|F_A|^2+|F_V|^2) + 4m_\ell^2 m_{B_c}^2|F_A|^2 + 2m_\ell(m_{B_c}^2 - m_{D_s}^2 + q^2)\mathrm{Re}(F_P F_A^*)\Big], \quad (8)$$

$$c_\ell = -\frac{G_F^2\alpha_{\rm EW}^2|V_{tb}V_{ts}^*|^2}{2^9\pi^5 m_{B_c}^3}\beta_\ell\sqrt{\lambda}\frac{\lambda\beta_\ell^2}{4}(|F_A|^2+|F_V|^2). \quad (9)$$

Here, the kinematical factor λ and the mass correction factor β_ℓ in the above equations are given by

$$\lambda = q^4 + m_{B_c}^4 + m_{D_s}^4 - 2(m_{B_c}^2 m_{D_s}^2 + m_{B_c}^2 q^2 + m_{D_s}^2 q^2),$$
$$\beta_\ell = \sqrt{1-4m_\ell^2/q^2}. \quad (10)$$

However, the explicit expressions of the form factors such as F_P, F_V and F_A are given as follows:

$$F_P = -m_\ell C_{10}\Big[f_+ - \frac{m_{B_c}^2 - m_{D_s}^2}{q^2}(f_0 - f_+)\Big], \quad (11)$$

$$F_V = C_9^{\rm eff} f_+ + \frac{2m_b}{m_{B_c}+m_{D_s}}C_7^{\rm eff} f_T, \quad (12)$$

$$F_A = C_{10} f_+. \quad (13)$$

We employ the Wilson coefficients at the renormalization scale $\mu = 4.8$ GeV as reported in Ref. [70].

Similarly, the transition amplitude for $B_c \to D_s^* \ell^+\ell^-$ decay channel can be obtained from the effective Hamiltonian given in the Eq. (1). The q^2 dependent differential branching ratio for $B_c \to D_s^*\ell^+\ell^-$ process is given as [71]

$$d\mathcal{BR}/dq^2 = \frac{d\Gamma/dq^2}{\Gamma_{\rm Total}} = \frac{\tau_{B_c}}{\hbar}\frac{1}{4}[3I_1^c + 6I_1^s - I_2^c - 2I_2^s], \quad (14)$$

where the q^2 dependent angular coefficients are given in Appendix B and the corresponding SM WCs at the renormalization scale $\mu = 4.8$ GeV are taken from [63]. In addition to this, we also define other prominent observables such as the forward-backward asymmetry $A_{\rm FB}$, the longitudinal polarization fraction F_L, and the angular observable P_5', which are given by [12]

$$F_L(q^2) = \frac{3I_1^c - I_2^c}{3I_1^c + 6I_1^s - I_2^c - 2I_2^s},$$
$$A_{\rm FB}(q^2) = \frac{3I_6}{3I_1^c + 6I_1^s - I_2^c - 2I_2^s},$$
$$\langle P_5'\rangle = \frac{\int_{\rm bin} dq^2 I_5}{2\sqrt{-\int_{\rm bin} dq^2 I_2^c \int_{\rm bin} dq^2 I_2^s}}. \quad (15)$$

To confirm the existence of the lepton universality violation, one can construct additional observables associated with the two different families of lepton pair which are quite sensitive to shed light into the windows of NP. The explicit expressions are given as below [13,72],

$$\langle Q_{F_L}\rangle = \langle F_L^\mu\rangle - \langle F_L^e\rangle, \qquad \langle Q_{A_{\rm FB}}\rangle = \langle A_{\rm FB}^\mu\rangle - \langle A_{\rm FB}^e\rangle,$$
$$\langle Q_5'\rangle = \langle P_5'^\mu\rangle - \langle P_5'^e\rangle. \quad (16)$$

Also we define the ratio of the branching ratios of μ to e transition in $B_c \to D_s^{(*)}\ell^+\ell^-$ decay modes as follows:

$$R_{D_s^{(*)}}(q^2) = \frac{\mathcal{BR}(B_c \to D_s^{(*)}\mu^+\mu^-)}{\mathcal{BR}(B_c \to D_s^{(*)}e^+e^-)}. \quad (17)$$

C. Differential decay distribution in $B_c \to D_s^{(*)}\nu\bar{\nu}$

The explicit study of $B_c \to D_s^{(*)}\nu\bar{\nu}$ processes involved with $b \to s\nu\bar{\nu}$ transitions are also quite important to search for NP beyond the SM as they are associated to $b \to s\ell^+\ell^-$ parton level by $SU(2)_L$ symmetry group. From the effective Hamiltonian given in Eq. (2), the differential decay rate for $B_c \to D_s^{(*)}\nu\bar{\nu}$ decay channel is given by [35,73]

$$\frac{d\mathcal{BR}(B_c \to D_s\nu\bar{\nu})_{\rm SM}}{dq^2} = \tau_{B_c} 3|N|^2 \frac{X_t^2}{s_w^4}\rho_{D_s}(q^2), \quad (18)$$

$$\frac{d\mathcal{BR}(B_c \to D_s^*\nu\bar{\nu})_{\rm SM}}{dq^2} = \tau_{B_c} 3|N|^2 \frac{X_t^2}{s_w^4}[\rho_{A_1}(q^2) + \rho_{A_{12}}(q^2) + \rho_V(q^2)], \quad (19)$$

where the factor 3 comes from the sum over neutrino flavors, and

$$N = V_{tb}V_{ts}^*\frac{G_F\alpha}{16\pi^2}\sqrt{\frac{m_{B_c}}{3\pi}} \quad (20)$$

is the normalization factor. The relevant rescaled form factors ρ_i given in the above equations are given below,

$$\rho_{D_s}(q^2) = \frac{\lambda_{D_s}^{3/2}(q^2)}{m_{B_c}^4}[f_+^{D_s}(q^2)]^2,$$
$$\rho_V(q^2) = \frac{2q^2\lambda_{D_s^*}^{3/2}(q^2)}{(m_{B_c}+m_{D_s^*})^2 m_{B_c}^4}[V(q^2)]^2,$$
$$\rho_{A_1}(q^2) = \frac{2q^2\lambda_{D_s^*}^{1/2}(q^2)(m_B+m_{D_s^*})^2}{m_{B_c}^4}[A_1(q^2)]^2,$$
$$\rho_{A_{12}}(q^2) = \frac{64m_{D_s^*}^2\lambda_{D_s^*}^{1/2}(q^2)}{m_{B_c}^2}[A_{12}(q^2)]^2. \quad (21)$$

The parameter λ is already defined for $B_c \to D_s$ transition in Eq. (10) and the pseudoscalar D_s is replaced by the vector meson D_s^* in $B_c \to D_s^*$ decays.

III. NEW PHYSICS ANALYSIS IN THE SCENARIO $C_9^{\mu\mu}(\mathrm{NP}) = -C_{10}^{\mu\mu}(\mathrm{NP})$

Assuming the NP exist only in the context of μ mode in $b \to s\ell^+\ell^-$ transition, it will contribute to more number of Lorentz structures. The new physics scenarios for the parton level $b \to s\mu^+\mu^-$ transition that account for NP contributions are given as [28,71]

$$\begin{aligned}
&(\mathrm{I}):\ C_9^{\mu\mu}(\mathrm{NP}) < 0,\\
&(\mathrm{II}):\ C_9^{\mu\mu}(\mathrm{NP}) = -C_{10}^{\mu\mu}(\mathrm{NP}) < 0,\\
&(\mathrm{III}):\ C_9^{\mu\mu}(\mathrm{NP}) = -C_9^{\prime\mu\mu}(\mathrm{NP}) < 0,\\
&(\mathrm{IV}):\ C_9^{\mu\mu}(\mathrm{NP}) = -C_{10}^{\mu\mu}(\mathrm{NP}) = C_9^{\prime\mu\mu}(\mathrm{NP}) = C_{10}^{\prime\mu\mu}(\mathrm{NP}) < 0,
\end{aligned} \quad (22)$$

where the unprimed couplings differ from the primed Wilson coefficients by their corresponding chiral operator as discussed in the previous section. Keeping in mind, as from the Ref. [74], only three out of ten leptoquarks, such as S_3, U_1, and U_3 can explain the $b \to s\mu^+\mu^-$ data as they have good fits under certain scenario. Among S_3, U_3, and U_1 leptoquarks, the U_1 leptoquark has no contribution to the couplings corresponding to the NP operator responsible for $b \to s\nu\bar{\nu}$ processes, whereas other two LQs are differentiated with a definite contributions to it. Hence, the effect from U_1 LQ is not taken into account in the present analysis. It is important to say that the remaining S_3 and U_3 LQs do not satisfy the scenarios I and III. On the other hand, in Ref. [75], it is also reported that Z' can contribute to both scenario I and II, whereas a vast majority of this model use the scenario II. Hence, the feasible environment to study both LQs and Z' simultaneously will be the scenario II: $C_9^{\mu\mu}(\mathrm{NP}) = -C_{10}^{\mu\mu}(\mathrm{NP})$. Many works have been studied in these scenarios in LQs [76–84] and in the presence of Z' [76,85–90]. Therefore, the purpose of this work is to concentrate on the scenario II: $C_9^{\mu\mu}(\mathrm{NP}) = -C_{10}^{\mu\mu}(\mathrm{NP})$ [75].

A. Leptoquark contribution

There are ten different leptoquark multiplets under the SM gauge group $SU(3)_C \times SU(2)_L \times U(1)_Y$ in the presence of dimension ≤ 4 operators [91] in which five multiplets include scalar (spin 0) and other halves are vectorial (spin 1) in nature under the Lorentz transformation. Among all, both the scalar triplet S^3 (Y = 1/3) and vector isotriplet U^3 (Y = −2/3) can explain the $b \to s\mu^+\mu^-$ and $b \to s\nu\bar{\nu}$ processes simultaneously. The relevant Lagrangian is given as follows [74]:

$$\mathcal{L}_S = y'_{\ell q}\bar{\ell}_L^c i\tau_2\vec{\tau}q_L S^3_{1/3} + \mathrm{H.c.},$$
$$\mathcal{L}_V = g'_{\ell q}\bar{\ell}_L\gamma_\mu\vec{\tau}q_L U^3_{-2/3} + \mathrm{H.c.}, \quad (23)$$

where the fermion currents in the above Lagrangian include the $SU(2)_L$ quark and lepton doublets "q_L" and "ℓ_L," respectively, and τ represent the Pauli matrices. Most importantly, the parameters $y'_{\ell q}$ and $g'_{\ell q}$ are the quark—lepton couplings associated with the corresponding leptoquarks. In particular, for this analysis, $y'^{\mu b(s)}_{\ell q}$ is the coupling of the leptoquark $S^3_{1/3}$ to the left-handed μ or ν_μ and a left-handed fermion field b (s). Similarly, $g'^{\mu b(s)}_{\ell q}$ is the coupling correspond to the leptoquark $U^3_{-2/3}$. On the other hand, for the parton level $b \to s\nu\bar{\nu}$ transitions, both $S^3_{1/3}$ and $U^3_{-2/3}$ LQs contribute differently as reported in Table I. Hence, the Wilson coefficient $C_L^{\nu\nu}$ associated with $b \to s\nu\bar{\nu}$ can be obtained by replacing $C_L^{\nu\nu} \to C_L^{\nu\nu} + C_L^{\nu\nu}(\mathrm{NP})$. In our paper, we consider the couplings $y'^{\mu b}_{\ell q}(y'^{\mu s}_{\ell q})^*$ and $g'^{\mu b}_{\ell q}(g'^{\mu s}_{\ell q})^*$ as real for the $S^3_{1/3}$ and $U^3_{-2/3}$ LQs respectively with the assumption of same mass for both the leptoquarks. The tree level Feynman diagram for these processes (left panel) mediated via LQ is shown in Fig. 1.

B. Nonuniversal Z' contribution

The extension of SM by an extra minimal $U(1)'$ gauge symmetry produces a neutral gauge boson the so-called Z' boson. It is the most obvious candidate that represents $b \to s\mu^+\mu^-$ in the NP scenario. However the main attraction of this model includes the flavor changing neutral current (FCNC) transition in the presence of new nonuniversal gauge boson Z' [92–94], which can contribute at tree

TABLE I. Contributions of the LQs–$S^3_{1/3}, U^3_{-2/3}$, and Z' to the Wilson coefficients. The normalization $\mathcal{R}(\mathcal{M}) \equiv \pi/(\sqrt{2}\alpha G_F V_{tb}V_{ts}^*(M_{LQ}(M_{Z'}))^2$ and $M_{LQ} = M_{Z'} = 1$ TeV.

NP model	$C_9^{\mu\mu}(\mathrm{NP})$	$C_{10}^{\mu\mu}(\mathrm{NP})$	$C_L^{\nu\nu}(\mathrm{NP})$
$S^3_{1/3}$	$\mathcal{R}y'^{\mu b}_{\ell q}(y'^{\mu s}_{\ell q})^*$	$-\mathcal{R}y'^{\mu b}_{\ell q}(y'^{\mu s}_{\ell q})^*$	$\frac{1}{2}\mathcal{R}y'^{\mu b}_{\ell q}(y'^{\mu s}_{\ell q})^*$
$U^3_{-2/3}$	$-\mathcal{R}g'^{\mu b}_{\ell q}(g'^{\mu s}_{\ell q})^*$	$\mathcal{R}g'^{\mu b}_{\ell q}(g'^{\mu s}_{\ell q})^*$	$-2\mathcal{R}g'^{\mu b}_{\ell q}(g'^{\mu s}_{\ell q})^*$
Z'	$-\mathcal{M}g_L^{bs}g_L^{\mu\mu}$	$\mathcal{M}g_L^{bs}g_L^{\mu\mu}$	$-\mathcal{M}g_L^{bs}g_L^{\nu\bar{\nu}}$

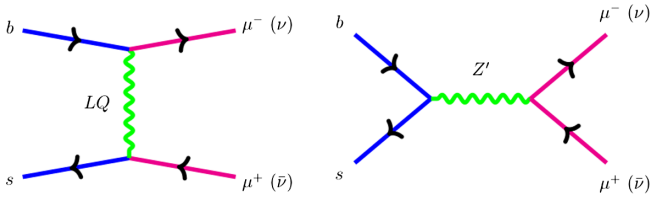

FIG. 1. The tree level contribution of the LQs and the Z' for $B_c \to D_s^{(*)}(\mu^+\mu^-, \nu\bar{\nu})$.

level given in Fig. 1 (right panel). After integrating out the heavy Z' the effective Lagrangian for 4 fermion operator is given as

$$\mathcal{L}_{Z'}^{\text{eff}} = -\frac{1}{2M_{Z'}^2} J'_\mu J^{\mu\prime}, \tag{24}$$

where the new current is given as

$$\begin{aligned} J^{\mu\prime} = &-g_{LL}^{\mu\mu}\bar{L}\gamma^\mu P_L L + g_{L(R)}^{\mu\mu}\bar{\mu}\gamma^\mu P_{L(R)}\mu \\ &+ g_L^{ij}\bar{\psi}_i\gamma^\mu P_L\psi_j + \text{H.c.}, \end{aligned} \tag{25}$$

where i and j are family index, $P_{L(R)}$ is the projection operator of left (right) chiral fermions and g_L^{ij} denote the left chiral coupling of Z' gauge boson. Now relevant interaction Lagrangian is given as

$$\mathcal{L}_{Z'}^{\text{eff}} = -\frac{g_L^{bs}}{m_{Z'}^2}(\bar{s}\gamma^\mu b)(\bar{\mu}\gamma^\mu(g_L^{\mu\mu}P_L + g_R^{\mu\mu}P_R)\mu). \tag{26}$$

Now, the modified Wilson coefficients in the presence of Z' model can be written as [25]

$$\begin{aligned} C_9^{\mu\mu}(\text{NP}) &= -\left[\frac{\pi}{\sqrt{2}G_F\alpha V_{tb}V_{ts}^*}\right]\frac{g_L^{bs}(g_L^{\mu\mu})}{m_{Z'}^2}, \\ C_{10}^{\mu\mu}(\text{NP}) &= \left[\frac{\pi}{\sqrt{2}G_F\alpha V_{tb}V_{ts}^*}\right]\frac{g_L^{bs}(g_L^{\mu\mu})}{m_{Z'}^2}, \end{aligned} \tag{27}$$

where g_L^{bs} is the coupling when b quark couple to s quark and $g_L^{\mu\mu}$ is the $\mu^+ - \mu^-$ coupling in the presence of new boson Z', and we have assumed $g_R^{\mu\mu} = 0$. Similarly for the $b \to s\nu\bar{\nu}$ transition, the NP contribution arising due to Z' is $C_L^{\nu\nu}(\text{NP}) = C_9^{\mu\mu}(\text{NP}) = -C_{10}^{\mu\mu}(\text{NP})$ [73]. From the neutrino trident production, $g_L^{\mu\mu} = 0.5$ has been considered in our paper [25,74,75]. The new parameter g_L^{bs} is taken to be real in our analysis.

IV. NUMERICAL ANALYSIS AND DISCUSSIONS

A. Input parameters

In this section, we report all the necessary input parameters used for our computational analysis. We consider the masses of mesons, quarks, Fermi coupling constant in the unit of GeV, and lifetime of B_c meson in the unit of second, CKM matrix element, and fine structure constant from Ref. [95]. We have adopted the lattice QCD method [45] and the relativistic quark model [40] based on quasipotential approach for the form factors of $B_c \to D_s$ and $B_c \to D_s^*$ transitions, respectively.

The form of the form factors for $B_c \to D_s$ transition in lattice QCD are given as follows:

$$f(q^2) = P(q^2)^{-1}\sum_{n=0}^{N_n} c^{(n)}\hat{z}^{(n,N_n)}, \tag{28}$$

where $N_n = 3$ and the q^2 dependent pole factor $P(q^2) = 1 - q^2/M_{\text{res}}^2$ ($M_{\text{res}} = 5.711$ (f_0) [96], 5.4158 ($f_{+,T}$) [95]). Using the Bourreley-Caprini-Lellouch (BCL) parametrization [97], the expressions of $\hat{z}_{0,+,T}^{n,N_n}$ are given as

$$\hat{z}_0^{n,N_n} = z^n, \qquad \hat{z}_{+,T}^{n,N_n} = z^n - \frac{n(-1)^{N_n+1-n}}{N_n+1}z^{N_n+1}. \tag{29}$$

Here, $z(q^2)$ is defined as

$$z(q^2) = \frac{\sqrt{t_+ - q^2} - \sqrt{t_+ - t_0}}{\sqrt{t_+ - q^2} + \sqrt{t_+ - t_0}}, \tag{30}$$

where $t_0 = 0$ and $t_+ = (m_{B(0^-)} + M_{K(0^-)})^2$ with the masses $M_{B(0^-)} = 5.27964$ and $M_{K(0^-)} = 0.497611$. The form factor coefficients $c^{(n)}$ are reported in Table II. For our error analysis, we employ 10% uncertainty in the form factor coefficients $c^{(n)}$. For all the omitted details, we refer to [45].

Similarly, the form factors for $B_c \to D_s^*$ transition are defined as

$$F(q^2) = \begin{cases} \dfrac{F(0)}{(1-\frac{q^2}{M^2})\left(1-\sigma_1\frac{q^2}{M_{B_s^*}^2}+\sigma_2\frac{q^4}{M_{B_s^*}^4}\right)}, & \text{for } F = \{V, A_0, T_1\} \\ \dfrac{F(0)}{\left(1-\sigma_1\frac{q^2}{M_{B_s^*}^2}+\sigma_2\frac{q^4}{M_{B_s^*}^4}\right)}, & \text{for } F = \{A_1, A_2, T_2, T_3\}. \end{cases} \tag{31}$$

TABLE II. The lattice QCD form factor coefficients $c^{(n)}$ for $B_c \to D_s$ transition [45] and the relativistic quark model form factors at $q^2 = 0$ and the corresponding fitted parameters σ_1 and σ_2 for $B_c \to D_s^*$ transition [40].

$B_c \to D_s$	$c^{(0)}$	$c^{(1)}$	$c^{(2)}$	$c^{(3)}$	$B_c \to D_s^*$	V	A_0	A_1	A_2	T_1	T_2	T_3
f_0	0.217	−0.220	1.300	−0.508	$F(0)$	0.182	0.070	0.089	0.110	0.085	0.085	0.051
f_+	0.217	−0.559	5.149	−0.217	σ_1	2.133	1.561	2.479	2.833	1.540	2.577	2.783
f_T	0.299	−1.501	3.579	−0.348	σ_2	1.183	0.192	1.686	2.167	0.248	1.859	2.170

Here, $M = M_{B_s}$ for $A_0(q^2)$, whereas $M = M_{B_s^*}$ is considered for all other form factors. We use $M_{B_s^*} = 5.4254$ GeV from the Ref. [95]. The related form factor input parameters for $B_c \to D_s^*$ are reported in the Table II. Similarly, we employ 10% uncertainty in the zero recoil momentum function $F(0)$ for our theoretical error in $B_c \to D_s^*$ form factors.

B. Fit results

To obtain the NP parameter space in the presence of Z' and LQs, we perform a naive χ^2 analysis with the available $b \to s\ell\ell$ experimental data. In the fit, we consider specifically the LHCb measurements of five different observables, such as R_K, R_{K^*}, P_5', $\mathrm{BR}(B_s \to \phi\mu\mu)$, and $\mathrm{BR}(B_s \to \mu^+\mu^-)$. Our fit include the latest measurements of R_K, $\mathrm{BR}(B_s \to \phi\mu\mu)$, and $\mathrm{BR}(B_s \to \mu^+\mu^-)$ as reported from LHCb in 2021. For our theoretical computation of the underlying observables, we refer to the lattice QCD form factors [70] for R_K and the form factors obtained from the combined analysis of LCSR + LQCD for $B \to K^*$ and $B_s \to \phi$ decay processes [1]. We define the χ^2 as

$$\chi^2(C_i^{\mathrm{NP}}) = \sum_i \frac{(\mathcal{O}_i^{\mathrm{th}}(C_{9,10}^{\mu\mu}(NP)) - \mathcal{O}_i^{\mathrm{exp}})^2}{(\Delta\mathcal{O}_i^{\mathrm{exp}})^2 + (\Delta\mathcal{O}_i^{\mathrm{sm}})^2}, \quad (32)$$

where $\mathcal{O}_i^{\mathrm{th}}$ represent the theoretical expressions, including the NP contributions and $\mathcal{O}_i^{\mathrm{exp}}$ are the experimental central values. The denominator includes 1σ uncertainties associated with the theoretical and experimental results. From our analysis, we obtain the best fit values and the corresponding 1σ range of the NP coupling strengths associated with Z', $S_{1/3}^3$, and $U_{-2/3}^3$ LQs, respectively, as shown in Table III. The best fit points for the NP couplings of Z' and LQs are obtained by minimizing the χ^2 variable. Similarly, to obtain the allowed 1σ range of each NP coupling, we impose $\chi^2 \leq 9.488$ constraint corresponding to 95% C.L. The minimum and maximum value of the 1σ range are given in Table III.

C. Interpretation of $B_c \to D_s^{(*)}(\mu^+\mu^-, \nu\bar{\nu})$ decays in the standard model and beyond

1. $B_c \to D_s^{(*)}\mu^+\mu^-$ decays

We perform NP studies of $B_c \to D_s^{(*)}\mu^+\mu^-$ decays in the presence of Z', $S_{1/3}^3$, and $U_{-2/3}^3$ LQs, which satisfy the $C_9^{\mu\mu}(NP) = -C_{10}^{\mu\mu}(NP)$ new physics scenario. Although the NP coupling strengths associated with the Z', $S_{1/3}^3$, and $U_{-2/3}^3$ LQs are different from each other, the contribution from the $C_9^{\mu\mu}(NP) = -C_{10}^{\mu\mu}(NP)$ new Wilson coefficients in $b \to s\ell^+\ell^-$ decays are same. Hence, we expect similar NP signature from Z', $S_{1/3}^3$, and $U_{-2/3}^3$ LQs in the underlying $B_c \to D_s^{(*)}\mu^+\mu^-$ decays. We study various observables such as the differential branching ratio, the forward backward asymmetry, the lepton polarization fraction, the LFU sensitive observables, including the ratio of the branching ratio $R_{D_s^{(*)}}$, and the difference of the observables associated with Q parameters, such as Q_{F_L}, $Q_{A_{\mathrm{FB}}}$, and Q_5' in the presence of SM as well as new physics. In Table IV, we report the central values and the corresponding standard deviation for all the observables in both SM and Z'/LQ new physics. Similarly in Figs. 2 and 3, we display the corresponding q^2 distribution plots as well as q^2 integrated bin wise plots for $B_c \to D_s\mu^+\mu^-$ and $B_c \to D_s^*\mu^+\mu^-$ processes, respectively. For the binned plots, we choose different bin sizes that are compatible with the LHCb experiments starting from [0.1, 0.98], [1.1, 2.5], [2.5, 4.0], [4.0, 6.0], and also [1.1, 6.0]. Similarly, for the q^2 distribution plots, we display the central lines and the corresponding 1σ error band for both SM and Z'/LQ new physics scenarios. The central lines are obtained by considering only the central values of all the input parameters, and the corresponding 1σ error bands are obtained by varying the form factors and the CKM matrix element within 1σ. In SM, we obtain the branching fraction to be $\mathcal{O}(10^{-7})$ for $B_c \to D_s^{(*)}\mu^+\mu^-$ decay channels. The detailed observations of our study are as follows:

(i) The q^2 dependency of the differential branching fraction for $B_c \to D_s^{(*)}\mu^+\mu^-$ decays are shown in the top—left panel of Figs. 2 and 3, respectively. We notice that the differential branching ratio is reduced in the presence of Z'/LQ new physics and the NP central line lies away from the SM uncertainty band for $B_c \to D_s\mu^+\mu^-$ decay. Although the Z'/LQ new physics contribution in $B_c \to D_s^*\mu^+\mu^-$ decay deviates from the SM central curve, it cannot be distinguished beyond the SM uncertainty; however, slight more deviation can be found at $q^2 > 4$ GeV^2. Moreover, partial overlapping of the SM and NP uncertainties can be noticed over the q^2. Similarly, in the top—right panel of Fig. 2 and bottom middle panel Fig. 3, we display the corresponding binned plots, respectively, for both the decay modes. We observe that for $B_c \to D_s\mu^+\mu^-$ decay in the all the bins the new physics contribution stand at $>1\sigma$ away from the SM. For the decay $B_c \to D_s^*\mu^+\mu^-$, however, the NP central values differ from the SM, but no such significant observations can be made.

TABLE III. The best-fit values and the corresponding 1σ ranges of the NP couplings associated with Z' and LQ models.

Values	Best fits	1σ range
NP models		
Z': $g_{bs}^{\mu\mu} \times 10^{-3}$	1.74	[0.11, 3.60]
$S_{1/3}^3$: $y_{\ell q}^{\prime\mu b}(y_{\ell q}^{\prime\mu s})^* \times 10^{-4}$	−8.70	[−15.50, −4.50]
$U_{-2/3}^3$: $g_{\ell q}^{\prime\mu b}(g_{\ell q}^{\prime\mu s})^* \times 10^{-4}$	8.70	[4.50, 15.50]

TABLE IV. The SM central value and the corresponding 1σ standard deviation of various physical observables in SM and in the presence of Z'/LQs for $B_c \to D_s^{(*)}\mu^+\mu^-$ decays.

Observable		[0.10, 0.98]	[1.1, 2.5]	[2.5, 4.0]	[4.0, 6.0]	[1.1, 6.0]
			$B_c \to D_s\mu^+\mu^-$			
BR $\times 10^{-7}$	SM	0.039 ± 0.007	0.072 ± 0.014	0.085 ± 0.015	0.126 ± 0.024	0.284 ± 0.052
	LQ/Z′	0.028 ± 0.005	0.053 ± 0.011	0.063 ± 0.013	0.095 ± 0.014	0.212 ± 0.036
$\langle R_{D_s}^{\mu e}\rangle$	SM	0.993 ± 0.025	1.001 ± 0.006	1.001 ± 0.004	1.001 ± 0.002	1.001 ± 0.003
	LQ/Z′	0.720 ± 0.020	0.737 ± 0.005	0.745 ± 0.004	0.753 ± 0.003	0.746 ± 0.003
			$B_c \to D_s^*\mu^+\mu^-$			
BR $\times 10^{-7}$	SM	0.018 ± 0.003	0.017 ± 0.007	0.029 ± 0.009	0.070 ± 0.024	0.116 ± 0.031
	LQ/Z′	0.017 ± 0.002	0.013 ± 0.005	0.022 ± 0.008	0.053 ± 0.013	0.088 ± 0.028
$\langle F_L\rangle$	SM	0.332 ± 0.122	0.707 ± 0.111	0.586 ± 0.129	0.454 ± 0.101	0.525 ± 0.093
	LQ/Z′	0.270 ± 0.099	0.682 ± 0.113	0.593 ± 0.095	0.461 ± 0.082	0.528 ± 0.101
$\langle A_{\rm FB}\rangle$	SM	0.163 ± 0.026	0.077 ± 0.060	-0.193 ± 0.054	-0.361 ± 0.064	-0.254 ± 0.051
	LQ/Z′	0.159 ± 0.017	0.137 ± 0.085	-0.151 ± 0.037	-0.341 ± 0.049	-0.220 ± 0.045
$\langle P_5'\rangle$	SM	0.528 ± 0.082	-0.477 ± 0.124	-0.869 ± 0.100	-0.936 ± 0.085	-0.842 ± 0.094
	LQ/Z′	0.573 ± 0.085	-0.337 ± 0.134	-0.825 ± 0.084	-0.924 ± 0.087	-0.803 ± 0.070
$\langle R_{D_s^*}^{\mu e}\rangle$	SM	0.979 ± 0.011	0.988 ± 0.005	0.990 ± 0.001	0.993 ± 0.000	0.992 ± 0.001
	LQ/Z′	0.924 ± 0.042	0.783 ± 0.020	0.752 ± 0.004	0.753 ± 0.004	0.757 ± 0.003
$\langle Q_{F_L}\rangle$	LQ/Z′	-0.057 ± 0.027	-0.018 ± 0.009	0.010 ± 0.001	0.008 ± 0.001	0.006 ± 0.001
$\langle Q_{A_{\rm FB}}\rangle$	LQ/Z′	-0.023 ± 0.012	0.058 ± 0.015	0.043 ± 0.017	0.020 ± 0.007	0.0034 ± 0.010
$\langle Q_5'\rangle$	LQ/Z′	0.073 ± 0.009	0.132 ± 0.016	0.038 ± 0.015	0.008 ± 0.006	0.032 ± 0.009

(ii) The ratio of branching ratio $R_{D_s^{(*)}}(q^2)$ is constant over the range $q^2 \in [0.1, 6.0]$ and is approximately equal to ~ 1. The uncertainties associated with this observable are almost zero both in SM as well as in the presence of NP contribution. The NP contribution from Z'/LQ is easily distinguishable from the SM contribution beyond the uncertainties at more than 5σ as shown in Figs. 2 and 3, respectively, for

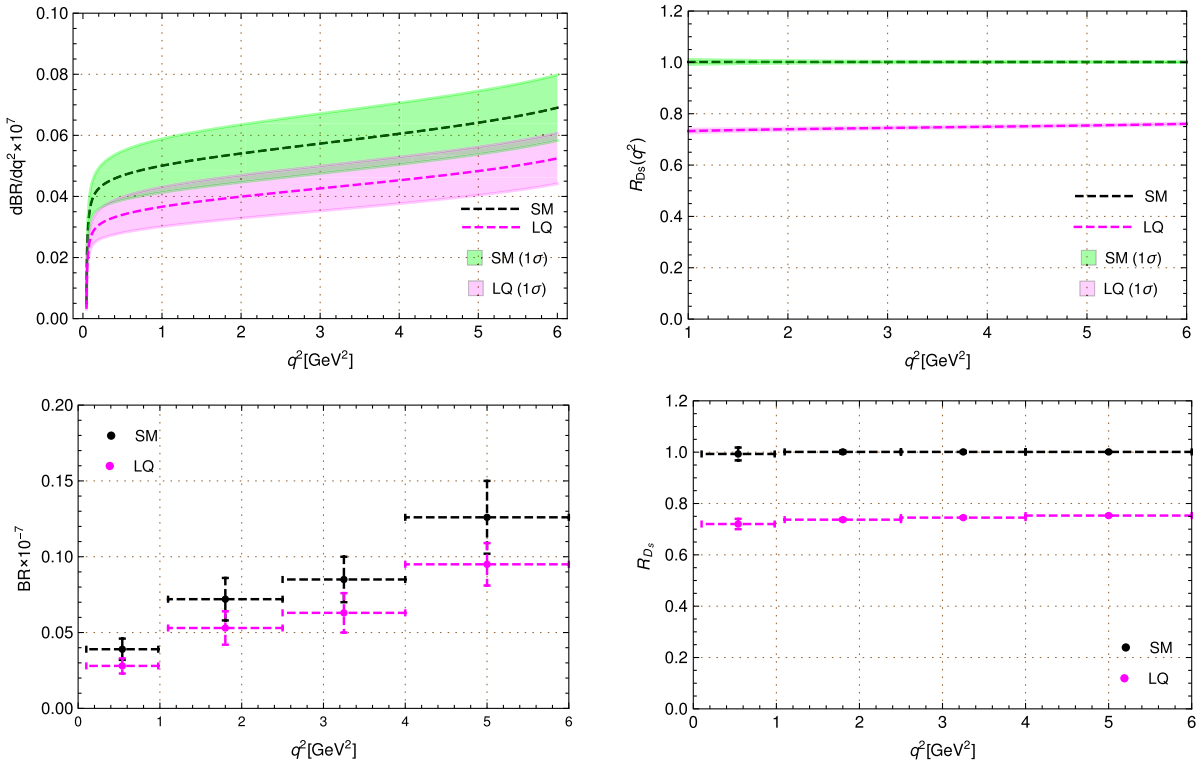

FIG. 2. The q^2 dependency and the bin wise distribution of the branching ratio and the ratio of branching ratio in $B_c \to D_s\mu^+\mu^-$ decays in SM and in the presence of Z'/LQs.

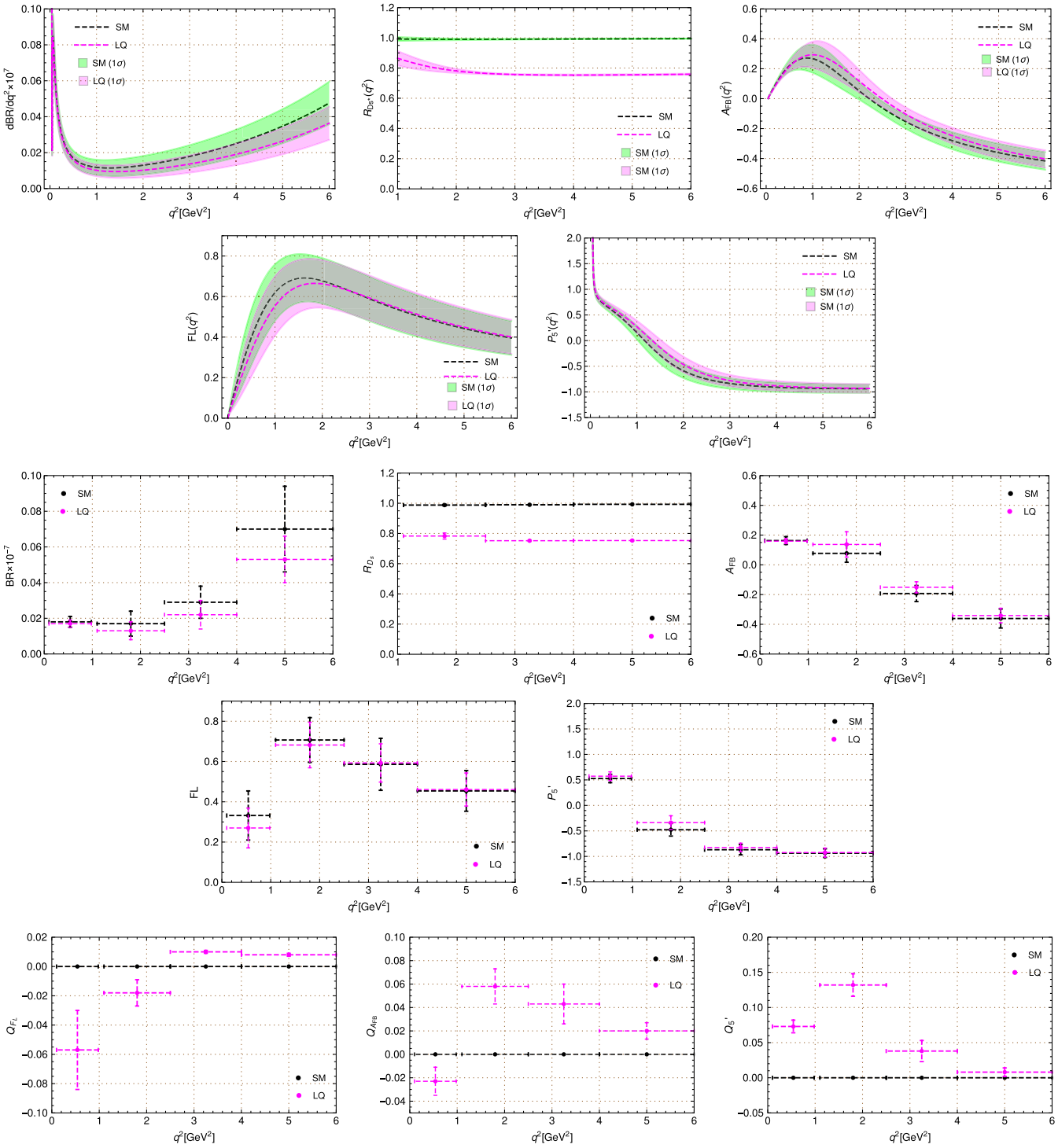

FIG. 3. The q^2 dependency and the bin wise distribution of various observables, such as the differential branching fraction, the ratio of branching ratio $R_{D_s^{(*)}}$, the forward backward asymmetry, the lepton polarization asymmetries, the angular observable P_5', and the Q parameters for $B_c \to D_s^*\mu^+\mu^-$ decays in SM and in the presence of Z'/LQs.

both the decays. However, the claim of 5σ deviation is observed only by considering the best fit points of Z'/LQ coupling strength and neglecting the corresponding experimental error of the measurement.

(iii) The q^2 distribution of the forward backward asymmetry $A_{\rm FB}(q^2)$ have a zero crossing at ∼2.2 GeV^2 in SM, which is different from the Z'/LQ new physics contribution crossing nearly at ∼2.5 GeV^2 as shown

in Fig. 3. Although there is overlapping between SM Z'/LQ error bands, the new zero crossing point from Z'/LQ NP is clearly distinguishable beyond the respective uncertainties. Similarly, in the binned plots, we observe that except for the bin [0.1,0.98], the $A_{\rm FB}$ values are shifted to higher values as compared to the SM estimations due to the Z'/LQ new physics contribution. However, in fact, in all q^2 bins, the Z'/LQ new physics spans less than 1σ deviation from the SM.

The Z'/LQ new physics contribution in the longitudinal polarization fraction $F_L(q^2)$ has shifted from the SM for $q^2 < 2$ GeV^2, while in the rest of q^2 region the NP contributions coincides with the SM contribution. No important observations can be drawn from $F_L(q^2)$.

For the angular observable $P_5'(q^2)$, in the region $q^2 \in [1.1, 2.5]$, the Z'/LQ new physics contribution can be clearly distinguished from the SM; however, it lies within the SM error band. Moreover, the error band corresponding to Z'/LQ NP almost overlaps with SM error band and cannot be distinguishable beyond the SM uncertainty. We do observe the zero crossing for $P_5'(q^2)$. In SM, we get the zero crossing at $\sim$1.2 GeV^2, which is different from the Z'/LQ new physics contribution observed at $\sim$1.4 GeV^2. However, the zero crossing corresponding to Z'/LQ NP cannot be clearly distinguished as it lies near the overlapping region of both the uncertainties.

(iv) The observables $\langle Q_{\rm FL}\rangle$, $\langle Q_{A_{\rm FB}}\rangle$ and $\langle Q_5'\rangle$ are purely sensitive to test the lepton flavor universality violation. The NP contribution in the Q observables can be clearly visualized. This is because of the reason that all Q's are zeros in SM, and hence, any nonzero contribution due the NP obviously justifies the beyond SM effects. From the Fig. 3, for $\langle Q_{\rm FL}\rangle$, we see that the uncertainties associated with the Z'/LQ new physics contribution in the lower q^2 bins such as [0.1, 0.98] and [1.1, 2.5] are huge, and hence, the deviation reduces nearly to 2σ whereas, for $q^2 > 2.5$ GeV^2, the Z'/LQ new physics contributions are clearly distinguishable at more than 5σ. In the case of $\langle Q_{A_{\rm FB}}\rangle$, the first three bins [0.1, 0.98], [1.1,2.5], and [2.5, 4.0] however show up to a 3σ deviation from the SM; the last bin [4.0, 6.0] is quite interesting with $> 3\sigma$ deviation. Similarly, for $\langle Q_5'\rangle$, except for the bin [4.0, 6.0], the rest of the bins are significantly distinguishable at more than 5σ from the SM predictions. In all the cases, we have neglected the experimental error.

2. $B_c \to D_s^{(*)}\nu\bar{\nu}$ decays

We know that the neutral semileptonic decays with the neutrinos in the final states are interesting due to the reduced hadronic uncertainties beyond the form factors. In fact, the $SU(2)_L$ gauge symmetry that treats the charged leptons $(\mu^+\mu^-)$ and neutral leptons $(\nu\bar{\nu})$ to be analogous invites one to examine the $b \to s\nu\bar{\nu}$ decays in the presence of various beyond the SM scenarios with the implications of available $b \to s\ell^+\ell^-$ experimental data. Since we are interested to find out the combined new physics solution which appears both in $b \to s(\ell^+\ell^-, \nu\bar{\nu})$ decays, we study $B_c \to D_s^{(*)}\nu\bar{\nu}$ decays in SM and also in the presence of Z', $S_{1/3}^3$, and $U_{-2/3}^3$ LQs, which satisfy the $C_9^{\mu\mu}(NP) = -C_{10}^{\mu\mu}(NP)$ scenario in $b \to s\ell^+\ell^-$ decays. This particular $C_9^{\mu\mu}(NP) = -C_{10}^{\mu\mu}(NP)$ scenario under similar Z'/LQ models has been discussed for the $B_c \to D_s^{(*)}\mu^+\mu^-$ decays in the previous section. The new physics contribution to the left-handed WC $C_L^{\nu\nu}$ associated with the operator $\mathcal{O}_L^{\nu\nu}$ in $b \to s\nu\bar{\nu}$ decays are related to the corresponding semileptonic WCs, such as $C_9^{\mu\mu}(NP)$ and $C_{10}^{\mu\mu}(NP)$. This contribution is different for Z', $S_{1/3}^3$, and $U_{-2/3}^3$ LQs as mentioned in Table I. Since we look for the new physics effects associated with left-handed neutrinos, the longitudinal polarization fraction appearing in $B_c \to D_s^*\nu\bar{\nu}$ decays have no effects beyond the SM; however, we only report the SM values for F_L in Table VI. We give predictions for the differential branching fraction in $B_c \to D_s^{(*)}\nu\bar{\nu}$ decays both in SM and in the presence of several NP models. We obtain the branching fraction for the underlying decays in SM of the $\mathcal{O}(10^{-6})$. In Table V, we report the corresponding branching ratios integrated over different q^2 bins in SM and in various NP scenarios. Similarly, in Fig. 4, we display the q^2 dependency of the differential branching ratio in SM, Z', $S_{1/3}^3$, and $U_{-2/3}^3$ LQs. In the figures, we display the central lines and the corresponding 1σ uncertainty bands, respectively, for SM and different NP contributions. The corresponding central lines are obtained by considering the central values of each input parameters, and the corresponding 1σ uncertainty band is obtained by varying the form factors and CKM matrix element within 1σ. For the different NP models that are constrained by the latest $b \to s\ell^+\ell^-$ data, we modify the SM WC $C_L^{\nu\nu}$ in $b \to s\nu\bar{\nu}$ decays accordingly as reported in Table IV. The detailed observations of our study are as follows:

(i) The q^2 dependency of $B_c \to D_s^{(*)}\nu\bar{\nu}$ decays for the whole kinematic range are displayed in the left panel of Fig. 4. We observe from the plots that the differential branching ratios are enhanced for all the NP contributions, and very interestingly, the $U_{-2/3}^3$ LQ show significant deviation from the SM curve and lie away from the SM error band. This is because of the reason that the $C_L^{\nu\nu}(NP)$—the left-handed new physics WC in $b \to s\nu\bar{\nu}$ decays for $U_{-2/3}^3$ LQ is rescaled to 2 times the $C_9^{\mu\mu}(NP) = -C_{10}^{\mu\mu}(NP)$ contribution; i.e., $C_L^{\nu\nu}(NP) = 2C_9^{\mu\mu}(NP) = -2C_{10}^{\mu\mu}(NP)$. Similarly,

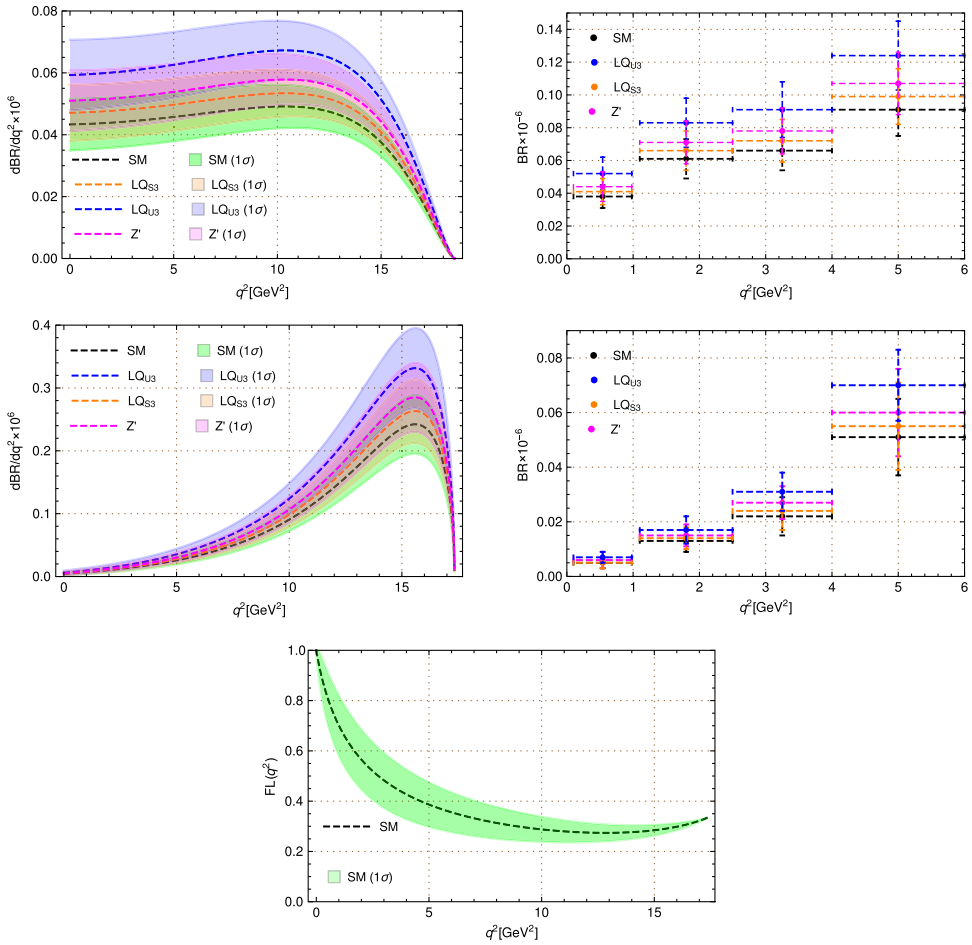

FIG. 4. The q^2 dependency and bin wise distribution of the branching ratios of $B_c \to D_s\nu\bar{\nu}$ (first row) and $B_c \to D_s^*\nu\bar{\nu}$ (second row) decays in the whole kinematic range in SM and in the presence of Z', $S_{1/3}^3$, and $U_{-2/3}^3$ LQs. Similarly, the q^2 dependency of the lepton polarization fraction of $B_c \to D_s^*\nu\bar{\nu}$ decays in SM is shown in the third row.

for the $S_{1/3}^3$ LQ, the $C_L^{\nu\nu}(NP) = (1/2)C_9^{\mu\mu}(NP) = -(1/2)C_{10}^{\mu\mu}(NP)$. On the other hand, for the Z' contribution, it is simply $C_L^{\nu\nu}(NP) = C_9^{\mu\mu}(NP) = -C_{10}^{\mu\mu}(NP)$ without any enhancement or reduction. To this end, we see that the $S_{1/3}^3$ LQ lie close to the SM, whereas Z' contribution lie at the 1σ boundary of the SM error band. Moreover, the error band of our feasible NP model associated with $U_{-2/3}^3$ LQ has distinguishable contributions beyond the uncertainties as compared to other NP models, such as $S_{1/3}^3$ LQ, and Z'. Similarly, on the right panel of Fig. 4, we display the bin wise distribution of the branching ratios only up to $q^2 = 6$ GeV^2 with the similar bin sizes as reported earlier. In Table V, we also have additional bin predictions that are not shown in figure. In all the bins, we do expect $> 1\sigma$ deviation for $U_{-2/3}^3$ LQ, almost 1σ deviation for Z', and $< 1\sigma$ for $S_{1/3}^3$ LQ.

(ii) The interesting fact about the new physics contribution in the longitudinal polarization fraction of $B_c \to D_s^*\nu\bar{\nu}$ decay is that it is sensitive only to the right-handed currents. Since in our analysis, the new physics arising from Z', $S_{1/3}^3$, and $U_{-2/3}^3$ LQs include only the left-handed contributions, the polarization fraction will not exhibit any additional new physics effects. This is because of the reason that when we define F_L as

$$F_L = F_L^{\rm SM}\frac{|C_L^{\nu\nu}|^2 + |C_R^{\nu\nu}|^2 - 2C_L^{\nu\nu}C_R^{\nu\nu}}{|C_L^{\nu\nu}|^2 + |C_R^{\nu\nu}|^2 - \kappa C_L^{\nu\nu}C_R^{\nu\nu}}, \quad (33)$$

where the $C_{L(R)}^{\nu\nu}$ are the Wilson coefficients associated with left- (right-)handed operators in $b \to s\nu\bar{\nu}$ decays, and κ is a form factor dependent parameter [35,73]. In the above equation for $C_R^{\nu\nu} = 0$, we obtain $F_L = F_L^{\rm SM}$, and hence, any new contribution in $C_L^{\nu\nu}$ will be canceled. Therefore, in this section, we report only the SM predictions for the F_L. The q^2 dependency of the longitudinal polarization fraction $F_L(q^2)$ for $B_c \to D_s^*\nu\bar{\nu}$ decay in the whole kinematic

TABLE V. The branching ratios of $B_c \to D_s^{(*)}\nu\bar{\nu}$ decays in different q^2 bins in SM and in the presence of Z', $S_{1/3}^3$, and $U_{-2/3}^3$ LQs.

q^2 bin	SM	LQ–S_3	LQ–U_3	Z'
		$\mathrm{BR}(B_c \to D_s\nu\bar{\nu}) \times 10^{-6}$		
[0.1–0.98]	0.038 ± 0.007	0.041 ± 0.008	0.052 ± 0.010	0.044 ± 0.009
[1.1–2.5]	0.061 ± 0.012	0.066 ± 0.012	0.083 ± 0.015	0.071 ± 0.013
[2.5–4.0]	0.066 ± 0.012	0.072 ± 0.013	0.091 ± 0.017	0.078 ± 0.014
[4.0–6.0]	0.091 ± 0.016	0.099 ± 0.017	0.124 ± 0.021	0.107 ± 0.019
[6.0–8.0]	0.094 ± 0.015	0.102 ± 0.016	0.129 ± 0.020	0.111 ± 0.017
[11–12.5]	0.072 ± 0.010	0.078 ± 0.010	0.099 ± 0.013	0.085 ± 0.011
$[15–q^2_{\mathrm{max}}]$	0.070 ± 0.008	0.076 ± 0.009	0.096 ± 0.012	0.082 ± 0.010
[1.1–6.0]	0.219 ± 0.040	0.238 ± 0.044	0.299 ± 0.057	0.257 ± 0.048
$[0–q^2_{\mathrm{max}}]$	0.758 ± 0.118	0.824 ± 0.130	1.038 ± 0.165	0.893 ± 0.145
		$\mathrm{BR}(B_c \to D_s^*\nu\bar{\nu}) \times 10^{-6}$		
[0.1–0.98]	0.004 ± 0.002	0.005 ± 0.002	0.006 ± 0.003	0.005 ± 0.002
[1.1–2.5]	0.013 ± 0.004	0.014 ± 0.004	0.017 ± 0.005	0.015 ± 0.004
[2.5–4.0]	0.022 ± 0.005	0.024 ± 0.008	0.031 ± 0.006	0.026 ± 0.006
[4.0–6.0]	0.051 ± 0.015	0.055 ± 0.011	0.070 ± 0.011	0.060 ± 0.010
[6.0–8.0]	0.0087 ± 0.020	0.094 ± 0.021	0.119 ± 0.018	0.102 ± 0.022
[11–12.5]	0.201 ± 0.045	0.218 ± 0.032	0.275 ± 0.034	0.236 ± 0.040
$[15–q^2_{\mathrm{max}}]$	0.481 ± 0.085	0.523 ± 0.092	0.659 ± 0.089	0.566 ± 0.100
[1.1–6.0]	0.087 ± 0.022	0.094 ± 0.025	0.119 ± 0.021	0.102 ± 0.020
$[0–q^2_{\mathrm{max}}]$	1.602 ± 0.313	1.741 ± 0.304	2.193 ± 0.285	1.886 ± 0.321

TABLE VI. The lepton polarization fraction of $B_c \to D_s^*\nu\bar{\nu}$ decays in different q^2 bins in SM.

q^2 bin	SM
$F_L(B_c \to D_s^*\nu\bar{\nu})$	
[0.1–0.98]	0.825 ± 0.074
[1.1–2.5]	0.603 ± 0.097
[2.5–4.0]	0.475 ± 0.105
[4.0–6.0]	0.389 ± 0.078
[6.0–8.0]	0.333 ± 0.064
[11–12.5]	0.277 ± 0.040
$[15–q^2_{\mathrm{max}}]$	0.301 ± 0.011
[1.1–6.0]	0.444 ± 0.101
$[0–q^2_{\mathrm{max}}]$	0.301 ± 0.040

range is displayed in the third row of Fig. 4. In the figure, we have shown only the central curve and the corresponding 1σ error band for SM. Similarly, in the Table VI, we report the SM mean and the corresponding standard deviation in various bins including from zero to maximum q^2 for which we obtain $F_L = 0.301 \pm 0.040$.

V. CONCLUSION

With the experimental data associated with $b \to s\ell^+\ell^-$ neutral current transition reported in the semileptonic $B \to (K, K^*)\mu^+\mu^-$ and $B_s \to \phi\mu^+\mu^-$ and also purely leptonic $B_s \to \mu^+\mu^-$ decay processes, we scrutinize the $B_c \to D_s^{(*)}\mu^+\mu^-$ and $B_c \to D_s^{(*)}\nu\bar{\nu}$ decays in the SM followed by the effects in the presence of leptoquark and Z' new physics models. Throughout the analysis, we have concentrated on the particular new physics scenario $C_9^{\mu\mu}(NP) = -C_{10}^{\mu\mu}(NP)$, where both the leptoquark and Z' models satisfy the particular condition. We obtain the Z' and LQ coupling strengths by fitting the five LHCb experimental data associated with $b \to s\ell^+\ell^-$ decays, including $R_{K^{(*)}}$, P_5', $\mathcal{B}(B_s \to \phi\mu^+\mu^-)$ and $\mathcal{B}(B_s \to \mu^+\mu^-)$. Notably, we include the latest updates of R_K, $\mathcal{B}(B_s \to \phi\mu^+\mu^-)$ and $\mathcal{B}(B_s \to \mu^+\mu^-)$ in our fit analysis. Interestingly, the new physics analysis pertaining to the $B_c \to D_s$ decay observables by using the lattice QCD form factor results are reported for the first time.

In the decays involving the charged leptons as a final state, we have performed a detailed study of various observables such as the differential branching fraction, the forward-backward asymmetry, the lepton polarization asymmetry, the angular observable P_5', and the ratio of branching ratios for $B_c \to D_s^{(*)}\mu^+\mu^-$ decays in SM and in the presence of Z'/LQ new physics. Simultaneously, the similar new physics contributions from Z' and LQs have been inspected in the branching ratios of $B_c \to D_s^{(*)}\nu\bar{\nu}$ decay processes. We observe from our analysis that the branching ratio is reduced due to Z'/LQ in the decays, which include the charged leptons as a final state, whereas in the processes involving neutrinos in the final state, the branching ratio is increased for Z', $S_{1/3}^3$, and $U_{-2/3}^3$ LQs. In fact, more significant deviation from the SM is found for

$U^3_{-2/3}$, particularly in $B_c \to D_s^{(*)}\nu\bar{\nu}$ decays. Moreover, the zero crossing of the forward-backward asymmetry in $B_c \to D_s^*\mu^+\mu^-$ process is shifted to higher q^2 value in the presence of Z'/LQ new physics. Similarly, the LFUV sensitive observables, including $R_{D_s^{(*)}}$ and the Q parameters, have significant deviations at more than 5σ from the SM in most of the q^2 bins. However, the claim of 5σ deviation can be made only with reference to the best fit point and neglecting the experimental error of the measurement. In addition, it is important to note that the NP contributions from Z', $S^3_{1/3}$, and $U^3_{-2/3}$ LQs in $B_c \to D_s^{(*)}\mu^+\mu^-$ decays are indistinguishable, whereas in the $B_c \to D_s^{(*)}\nu\bar{\nu}$ case, all the three new physics contributions are clearly distinguished from one another. Having said that, the decay modes $B_c \to D_s^{(*)}(\mu^+\mu^-, \nu\bar{\nu})$ mediated by $b \to s(\ell^+\ell^-, \nu\bar{\nu})$ transition have received very less attention than the current ongoing study in $B_{(s)} \to (K, K^*, \phi)\ell^+\ell^-$ processes. Hence, the combined study of particular decays $B_c \to D_s^{(*)}\mu^+\mu^-$ and $B_c \to D_s^{(*)}\nu\bar{\nu}$ will certainly help us in identifying the possible new physics signatures in both $b \to s\ell^+\ell^-$ and $b \to s\nu\bar{\nu}$ decays. Moreover, the improved estimations of the various form factors corresponding to the $B_c \to D_s$ and $B_c \to D_s^*$ transitions will be crucial in the near future to understand the nature of NP. In addition to this, more data samples from the experiments are also required to visualize various observables in the $B_c \to D_s^{(*)}(\ell^+\ell^-, \nu\bar{\nu})$ decay processes, and in particular, the more experimental studies pertaining to $b \to s\nu\bar{\nu}$ decays can assist to identify the various new physics Lorentz structures.

ACKNOWLEDGMENTS

M. K. M. acknowledges INSPIRE fellowship Division, Department of Science and Technology, Government of India for the financial support with ID No. 160303. N. R. would like to thank CSIR for the financial help in this work.

APPENDIX A: FORM FACTORS FOR $B_c \to D_s^{(*)}\ell\ell(\ell = e, \mu)$

The hadronic matrix elements for the exclusive $B_c \to D_s$ transition in terms of form factors is given by [45]

$$\begin{aligned} J_\mu &= \langle D_s|\bar{s}\gamma^\mu b|B_c\rangle \\ &= f_+(q^2)\left[p^\mu_{B_c} + p^\mu_{D_s} - \frac{M^2_{B_c} - M^2_{D_s}}{q^2}q^\mu\right] \\ &\quad + f_0(q^2)\frac{M^2_{B_c} - M^2_{D_s}}{q^2}q^\mu, \\ J^T_\mu &= \langle D_s|\bar{s}\sigma^{\mu\nu}q_\nu b|B_c\rangle \\ &= \frac{if_T(q^2)}{M_{B_c} + M_{D_s}}[q^2(p^\mu_{B_c} + p^\mu_{D_s} - (M^2_{B_c} - M^2_{D_s})q^\mu], \end{aligned} \tag{A1}$$

where $q = p_{B_c} - p_{D_s}$ and the form factors given above the expression satisfy the following relations:

$$\begin{aligned} f_+(0) &= f_0, \\ f_0(q^2) &= f_+(q^2) + \frac{q^2}{m^2_{B_c} - m^2_{D_s}}f_-(q^2). \end{aligned} \tag{A2}$$

Similarly, for the $B_c \to D_s^*$ transition, the hadronic matrix elements can be given in terms of the form factors as [40]

$$\begin{aligned} \langle D_s^*|\bar{s}\gamma^\mu b|B_c\rangle &= \frac{2iV(q^2)}{M_{B_c} + M_{D_s^*}}\epsilon^{\mu\nu\rho\sigma}\epsilon^*_\nu p_{B_{c\rho}} p_{D^*_{s\sigma}}, \\ \langle D_s^*|\bar{s}\gamma^\mu\gamma_5 b|B_c\rangle &= 2M_{D_s^*}A_0(q^2)\frac{\epsilon^*\cdot q}{q^2}q^\mu + (M_{B_c} + M_{D_s^*})A_1(q^2)\left(\epsilon^{*\mu} - \frac{\epsilon^*\cdot q}{q^2}q^\mu\right) \\ &\quad - A_2(q^2)\frac{\epsilon^*\cdot q}{M_{B_c} + M_{D_s^*}}\left[p^\mu_{B_c} + p^\mu_{D_s^*} - \frac{M^2_{B_c} - M^2_{D_s^*}}{q^2}q^\mu\right], \\ \langle D_s^*|\bar{s}i\sigma^{\mu\nu}q_\nu b|B_c\rangle &= 2T_1(q^2)\epsilon^{\mu\nu\rho\sigma}\epsilon^*_\nu p_{B_{c\rho}} p_{D^*_{s\sigma}}, \\ \langle D_s^*|\bar{s}i\sigma^{\mu\nu}\gamma_5 q_\nu b|B_c\rangle &= T_2(q^2)[(M^2_{B_c} - M^2_{D_s^*})\epsilon^{*\mu} - (\epsilon^*\cdot q)(p^\mu_{B_c} + p^\mu_{D_s^*})] \\ &\quad + T_3(q^2)(\epsilon^*\cdot q)\left[q^\mu - \frac{q^2}{M^2_{B_c} - M^2_{D_s^*}}(p^\mu_{B_c} + p^\mu_{D_s^*})\right], \end{aligned} \tag{A3}$$

where $q^\mu = (p^\mu_B - p^\mu_{D_s})$ is the four momentum transfer and ϵ_μ is polarization vector of the D_s^* meson.

APPENDIX B: ANGULAR COEFFICIENTS

The q^2 dependent angular coefficients required for $B_c \to D_s^* \ell\ell(\ell = \mu)$ processes are given as follows:

$$
\begin{aligned}
I_1^c &= (|A_{L0}|^2 + |A_{R0}|^2) + 8\frac{m_l^2}{q^2}\mathrm{Re}[A_{L0}A_{R0}^*] + 4\frac{m_l^2}{q^2}|A_t|^2,\\
I_2^c &= -\beta_l^2(|A_{L0}|^2 + |A_{R0}|^2),\\
I_1^s &= \frac{3}{4}[|A_{L\perp}|^2 + |A_{L\parallel}|^2 + |A_{R\perp}|^2 + |A_{R\parallel}|^2]\left(1 - \frac{4m_l^2}{3q^2}\right) + \frac{4m_l^2}{q^2}\mathrm{Re}[A_{L\perp}A_{R\perp}^* + A_{L\parallel}A_{R\parallel}^*],\\
I_2^s &= \frac{1}{4}\beta_l^2[|A_{L\perp}|^2 + |A_{L\parallel}|^2 + |A_{R\perp}|^2 + |A_{R\parallel}|^2],\\
I_3 &= \frac{1}{2}\beta_l^2[|A_{L\perp}|^2 - |A_{L\parallel}|^2 + |A_{R\perp}|^2 - |A_{R\parallel}|^2],\\
I_4 &= \frac{1}{\sqrt{2}}\beta_l^2[\mathrm{Re}(A_{L0}A_{L\parallel}^*) + \mathrm{Re}(A_{R0}A_{R\parallel}^*)],\\
I_5 &= \sqrt{2}\beta_l[\mathrm{Re}(A_{L0}A_{L\perp}^*) - \mathrm{Re}(A_{R0}A_{R\perp}^*)],\\
I_6 &= 2\beta_l[\mathrm{Re}(A_{L\parallel}A_{L\perp}^*) - \mathrm{Re}(A_{R\parallel}A_{R\perp}^*)],\\
I_7 &= \sqrt{2}\beta_l[\mathrm{Im}(A_{L0}A_{L\parallel}^*) - \mathrm{Im}(A_{R0}A_{R\parallel}^*)],\\
I_8 &= \frac{1}{\sqrt{2}}\beta_l^2[\mathrm{Im}(A_{L0}A_{L\perp}^*) + \mathrm{Im}(A_{R0}A_{R\perp}^*)],\\
I_9 &= \beta_l^2[\mathrm{Im}(A_{L\parallel}A_{L\perp}^*) + \mathrm{Im}(A_{R\parallel}A_{R\perp}^*)],
\end{aligned}
\tag{B1}
$$

where $\beta_\ell = \sqrt{1 - 4m_\ell^2/q^2}$. According to Ref. [69], the transversity amplitude in terms of form factors and Wilson coefficients are given as

$$
\begin{aligned}
A_{L0} &= N\frac{1}{2m_{D_s^*}\sqrt{q^2}}\left\{(C_9^{\mathrm{eff}} - C_{10})\left[(m_{B_s}^2 - m_{D_s^*}^2 - q^2)(m_{B_s} + m_{D_s^*})A_1 - \frac{\lambda}{m_{B_s} + m_{D_s^*}}A_2\right]\right.\\
&\quad \left. + 2m_b C_7^{\mathrm{eff}}\left[(m_{B_s}^2 + 3m_{D_s^*}^2 - q^2)T_2 - \frac{\lambda}{m_{B_s}^2 - m_{D_s^*}^2}T_3\right]\right\},\\
A_{L\perp} &= -N\sqrt{2}\left[(C_9^{\mathrm{eff}} - C_{10})\frac{\sqrt{\lambda}}{m_{B_s} + m_{D_s^*}}V + \frac{\sqrt{\lambda}2m_b C_7^{\mathrm{eff}}}{q^2}T_1\right],\\
A_{L\parallel} &= N\sqrt{2}\left[(C_9^{\mathrm{eff}} - C_{10})(m_{B_s} + m_{D_s^*})A_1 + \frac{2m_b C_7^{\mathrm{eff}}(m_{B_s}^2 - m_{D_s^*}^2)}{q^2}T_2\right],\\
A_{Lt} &= N(C_9^{\mathrm{eff}} - C_{10})\frac{\sqrt{\lambda}}{\sqrt{q^2}}A_0,
\end{aligned}
\tag{B2}
$$

where $\lambda = (m_{B_c}^4 + m_{D_s}^4 + q^4 - 2(m_{B_c}^2 m_{D_s}^2 + m_{D_s}^2 q^2 + q^2 m_{B_c}^2)$ and N, the normalization constant, which is defined as

$$
N = \left[\frac{G_F^2\alpha_{em}^2}{3\cdot 2^{10}\pi^5 m_{B_s}^3}|V_{tb}V_{ts}^*|^2 q^2\sqrt{\lambda}\left(1 - \frac{4m_l^2}{q^2}\right)^{1/2}\right]^{1/2}. \tag{B3}
$$

The right chiral component A_{Ri} of the transversity amplitudes can be obtained by replacing A_{Li} by $A_{Li}|_{C_{10}\to -C_{10}}(i = 0, \parallel, \perp, t)$.

[1] A. Bharucha, D. M. Straub, and R. Zwicky, $B \to V\ell^+\ell^-$ in the Standard Model from light-cone sum rules, J. High Energy Phys. 08 (2016) 098.

[2] R. Aaij *et al.*, Test of lepton universality with $B^0 \to K^{*0}\ell^+\ell^-$ decays, J. High Energy Phys. 08 (2017) 055.

[3] R. Aaij *et al.*, Measurement of *CP*-Averaged Observables in the $B^0 \to K^{*0}\mu^+\mu^-$ Decay, Phys. Rev. Lett. **125**, 011802 (2020).

[4] A. Abdesselam *et al.*, Test of Lepton-Flavor Universality in $B \to K^*\ell^+\ell^-$ Decays at Belle, Phys. Rev. Lett. **126**, 161801 (2021).

[5] M. Bordone, G. Isidori, and A. Pattori, On the Standard Model predictions for R_K and R_{K^*}, Eur. Phys. J. C **76**, 440 (2016).

[6] G. Hiller and F. Kruger, More model-independent analysis of $b \to s$ processes, Phys. Rev. D **69**, 074020 (2004).

[7] M. Aaboud *et al.*, Angular analysis of $B_d^0 \to K^*\mu^+\mu^-$ decays in pp collisions at $\sqrt{s} = 8$ TeV with the ATLAS detector, J. High Energy Phys. 10 (2018) 047.

[8] R. Aaij *et al.*, Measurement of Form-Factor-Independent Observables in the Decay $B^0 \to K^{*0}\mu^+\mu^-$, Phys. Rev. Lett. **111**, 191801 (2013).

[9] R. Aaij *et al.*, Angular analysis of the $B^0 \to K^{*0}\mu^+\mu^-$ decay using 3 fb^{-1} of integrated luminosity, J. High Energy Phys. 02 (2016) 104.

[10] CMS Collaboration, Measurement of the P_1 and P_5' angular parameters of the decay $B \to K^*\mu^+\mu^-$ in proton proton collisions at $\sqrt{s} = 8$ TeV, 2017.

[11] A. Abdesselam *et al.*, Angular analysis of $B^0 \to K^*(892)^0\ell^+\ell^-$, in *proceedings of LHC Ski 2016: A First Discussion of 13 TeV Results, Obergurgl, Austria* (2016), https://inspirehep.net/literature/1446979.

[12] S. Descotes-Genon, J. Matias, M. Ramon, and J. Virto, Implications from clean observables for the binned analysis of $B- > K*\mu^+\mu^-$ at large recoil, J. High Energy Phys. 01 (2013) 048.

[13] S. Descotes-Genon, T. Hurth, J. Matias, and J. Virto, Optimizing the basis of $B \to K^*ll$ observables in the full kinematic range, J. High Energy Phys. 05 (2013) 137.

[14] S. Descotes-Genon, L. Hofer, J. Matias, and J. Virto, On the impact of power corrections in the prediction of $B \to K^*\mu^+\mu^-$ observables, J. High Energy Phys. 12 (2014) 125.

[15] R. Aaij *et al.*, Test of lepton universality in beauty-quark decays, Nat. Phys. **18**, 277 (2022).

[16] R. Aaij *et al.*, Search for Lepton-Universality Violation in $B^+ \to K^+\ell^+\ell^-$ Decays, Phys. Rev. Lett. **122**, 191801 (2019).

[17] R. Aaij *et al.*, Branching Fraction Measurements of the Rare $B_s^0 \to \phi\mu^+\mu^-$ and $B_s^0 \to f_2'(1525)\mu^+\mu^-$ Decays, Phys. Rev. Lett. **127**, 151801 (2021).

[18] R. Aaij *et al.*, Differential branching fraction and angular analysis of the decay $B_s^0 \to \phi\mu^+\mu^-$, J. High Energy Phys. 07 (2013) 084.

[19] R. Aaij *et al.*, Angular analysis and differential branching fraction of the decay $B_s^0 \to \phi\mu^+\mu^-$, J. High Energy Phys. 09 (2015) 179.

[20] J. Aebischer, J. Kumar, P. Stangl, and D. M. Straub, A global likelihood for precision constraints and flavour anomalies, Eur. Phys. J. C **79**, 509 (2019).

[21] J. Grygier *et al.*, Search for $B \to h\nu\bar{\nu}$ decays with semileptonic tagging at Belle, Phys. Rev. D **96**, 091101 (2017); **97**, 099902(A) (2018).

[22] J. P. Lees *et al.*, Search for $B \to K^{(*)}\nu\bar{\nu}$ and invisible quarkonium decays, Phys. Rev. D **87**, 112005 (2013).

[23] T. E. Browder, N. G. Deshpande, R. Mandal, and R. Sinha, Impact of $B \to K\nu\bar{\nu}$ measurements on beyond the Standard Model theories, Phys. Rev. D **104**, 053007 (2021).

[24] Y. Li, J. Hua, and K.-C. Yang, $B \to K_1\ell^+\ell^-$ decays in a family non-universal Z' model, Eur. Phys. J. C **71**, 1775 (2011).

[25] Z.-R. Huang, M. A. Paracha, I. Ahmed, and C.-D. Lü, Testing leptoquark and Z' models via $B \to K_1(1270, 1400)\mu^+\mu^-$ decays, Phys. Rev. D **100**, 055038 (2019).

[26] F. Falahati and A. Zahedidareshouri, Forward-backward asymmetries of $\bar{B} \to \bar{K}_1(1270)\ell^+\ell^-$ and $\bar{B} \to \bar{K}^*\ell^+\ell^-$ transitions in two Higgs doublet model, Phys. Rev. D **90**, 075002 (2014).

[27] I. Ahmed, M. Ali Paracha, and M. J. Aslam, Model independent analysis of the forward-backward asymmetry for the $B \to K_1\mu^+\mu^-$ decay, Eur. Phys. J. C **71**, 1521 (2011).

[28] B. Capdevila, A. Crivellin, S. Descotes-Genon, J. Matias, and J. Virto, Patterns of new physics in $b \to s\ell^+\ell^-$ transitions in the light of recent data, J. High Energy Phys. 01 (2018) 093.

[29] V. Bashiry, Lepton polarization in $B \to K_1\ell^+\ell^-$ decays, J. High Energy Phys. 06 (**2009**) 062.

[30] R. N. Faustov and V. O. Galkin, Rare $B \to \pi l\bar{l}$ and $B \to \rho l\bar{l}$ decays in the relativistic quark model, Eur. Phys. J. C **74**, 2911 (2014).

[31] W.-F. Wang and Z.-J. Xiao, The semileptonic decays $B/B_s \to (\pi, K)(\ell^+\ell^-, \ell\nu, \nu\bar{\nu})$ in the perturbative QCD approach beyond the leading-order, Phys. Rev. D **86**, 114025 (2012).

[32] R.-H. Li, C.-D. Lu, and W. Wang, Branching ratios, forward-backward asymmetries and angular distributions of $B \to K_2^*l^+l^-$ in the standard model and new physics scenarios, Phys. Rev. D **83**, 034034 (2011).

[33] N. Rajeev, N. Sahoo, and R. Dutta, Angular analysis of $B_s \to f_2'(1525)(\to K^+K^-)\mu^+\mu^-$ decays as a probe to lepton flavor universality violation, Phys. Rev. D **103**, 095007 (2021).

[34] C. Bobeth, A. J. Buras, F. Kruger, and J. Urban, QCD corrections to $\bar{B} \to X_{d,s}\nu\bar{\nu}$, $\bar{B}_{d,s} \to \ell^+\ell^-$, $K \to \pi\nu\bar{\nu}$ and $K_L \to \mu^+\mu^-$ in the MSSM, Nucl. Phys. **B630**, 87 (2002).

[35] W. Altmannshofer, A. J. Buras, D. M. Straub, and M. Wick, New strategies for new physics search in $B \to K^*\nu\bar{\nu}$, $B \to K\nu\bar{\nu}$ and $B \to X_s\nu\bar{\nu}$ decays, J. High Energy Phys. 04 (2009) 022.

[36] S. Descotes-Genon, S. Fajfer, J. F. Kamenik, and M. Novoa-Brunet, Implications of $b \to s\mu\mu$ anomalies for future measurements of $B \to K^{(*)}\nu\bar{\nu}$ and $K \to \pi\nu\bar{\nu}$, Phys. Lett. B **809**, 135769 (2020).

[37] S. Fajfer, N. Košnik, and L. Vale Silva, Footprints of leptoquarks: from $R_{K^{(*)}}$ to $K \to \pi\nu\bar{\nu}$, Eur. Phys. J. C **78**, 275 (2018).

[38] Y. Li and C.-D. Lü, Recent anomalies in B physics, Sci. Bull. **63**, 267 (2018).

[39] A. K. Alok, A. Dighe, S. Gangal, and D. Kumar, Predictions for $B_s \to \bar{K}^*\ell\ell$ in non-universal Z' models, Eur. Phys. J. C **80**, 682 (2020).

[40] D. Ebert, R. N. Faustov, and V. O. Galkin, Rare semileptonic decays of B and B_c mesons in the relativistic quark model, Phys. Rev. D **82**, 034032 (2010).

[41] C. Q. Geng, C.-W. Hwang, and C. C. Liu, Study of rare $B_c^+ \to D_{d,s} +$ lepton anti-lepton decays, Phys. Rev. D **65**, 094037 (2002).

[42] H.-M. Choi, Light-front quark model analysis of the exclusive rare $B_c \to D_{(s)}(\ell^+\ell^-, \nu_\ell\bar{\nu}_\ell)$ decays, Phys. Rev. D **81**, 054003 (2010).

[43] K. Azizi, F. Falahati, V. Bashiry, and S. M. Zebarjad, Analysis of the rare $B(c) \to D^*(s,d)l^+l^-$ decays in QCD, Phys. Rev. D **77**, 114024 (2008).

[44] A. Issadykov, M. A. Ivanov, and G. Nurbakova, Semileptonic decays of B_c mesons into charmonium states, EPJ Web Conf. **158**, 03002 (2017).

[45] L. J. Cooper, C. T. H. Davies, and M. Wingate, Form factors for the processes $B_c^+ \to D^0\ell^+\nu_\ell$ and $B_c^+ \to D_s^+\ell^+\ell^-(\nu\bar{\nu})$ from lattice QCD, Phys. Rev. D **105**, 014503 (2022).

[46] R. Dutta, Model independent analysis of new physics effects on $B_c \to (D_s, D_s^*)\mu^+\mu^-$ decay observables, Phys. Rev. D **100**, 075025 (2019).

[47] L.-x. Lu, Z.-j. Xiao, S.-w. Wang, and Z.-q. Zhang, The rare decay $B_c \to D_s^*\mu^+\mu^-$ in a family non-nuiversal model, Commun. Theor. Phys. **59**, 187 (2013).

[48] P. Maji, S. Mahata, P. Nayek, S. Biswas, and S. Sahoo, Investigation of rare semileptonic $B_c \to (D_{s,d}^{(*)})\mu^+\mu^-$ decays with non-universal Z' effect, Chin. Phys. C **44**, 073106 (2020).

[49] W.-F. Wang, X. Yu, C.-D. Lü, and Z.-J. Xiao, Semileptonic decays $B_c^+ \to D_{(s)}^{(*)}(l^+l^-, l^+l^-)$, in the perturbative QCD approach, Phys. Rev. D **90**, 094018 (2014).

[50] F. Abe *et al.*, Observation of the B_c Meson in $p\bar{p}$ Collisions at $\sqrt{s} = 1.8$ TeV, Phys. Rev. Lett. **81**, 2432 (1998).

[51] D.-s. Du and Z. Wang, Predictions of the standard model for $B_c^\pm$ weak decays, Phys. Rev. D **39**, 1342 (1989).

[52] C.-H. Chang and Y.-Q. Chen, The hadronic production of the B(c) meson at Tevatron, CERN LHC and SSC, Phys. Rev. D **48**, 4086 (1993).

[53] K.-m. Cheung, B(c) Mesons Production at Hadron Colliders by Heavy Quark Fragmentation, Phys. Rev. Lett. **71**, 3413 (1993).

[54] E. Braaten, K.-m. Cheung, and T. C. Yuan, Perturbative QCD fragmentation functions for B_c and B_c * production, Phys. Rev. D **48**, R5049 (1993).

[55] S. Stone, The goals and techniques of BTEV and LHC-B, Proc. Int. Sch. Phys. Fermi **137**, 559 (1998).

[56] I. P. Gouz, V. V. Kiselev, A. K. Likhoded, V. I. Romanovsky, and O. P. Yushchenko, Prospects for the B_c studies at LHCb, Phys. At. Nucl. **67**, 1559 (2004).

[57] M. Pepe Altarelli and F. Teubert, B physics at LHCb, Int. J. Mod. Phys. A **23**, 5117 (2008).

[58] F. Abudinén *et al.*, Search for $B^+ \to K^+\nu\bar{\nu}$ Decays Using an Inclusive Tagging Method at Belle II, Phys. Rev. Lett. **127**, 181802 (2021).

[59] A. J. Buras and M. Munz, Effective Hamiltonian for $B \to X_s e^+e^-$ beyond leading logarithms in the NDR and HV schemes, Phys. Rev. D **52**, 186 (1995).

[60] D. Melikhov, N. Nikitin, and S. Simula, Rare exclusive semileptonic $b \to s$ transitions in the standard model, Phys. Rev. D **57**, 6814 (1998).

[61] G. Buchalla, A. J. Buras, and M. E. Lautenbacher, Weak decays beyond leading logarithms, Rev. Mod. Phys. **68**, 1125 (1996).

[62] D. Bardhan, P. Byakti, and D. Ghosh, Role of tensor operators in R_K and R_{K^*}, Phys. Lett. B **773**, 505 (2017).

[63] A. Ali, P. Ball, L. T. Handoko, and G. Hiller, A comparative study of the decays $B \to (K, K^*)\ell^+\ell^-$ in standard model and supersymmetric theories, Phys. Rev. D **61**, 074024 (2000).

[64] A. Khodjamirian, T. Mannel, A. A. Pivovarov, and Y. M. Wang, Charm-loop effect in $B \to K^{(*)}\ell^+\ell^-$ and $B \to K^*\gamma$, J. High Energy Phys. 09 (2010) 089.

[65] A. Khodjamirian, T. Mannel, and Y. M. Wang, $B \to K\ell^+\ell^-$ decay at large hadronic recoil, J. High Energy Phys. 02 (2013) 010.

[66] C. Bobeth, M. Chrzaszcz, D. van Dyk, and J. Virto, Long-distance effects in $B \to K^*\ell\ell$ from analyticity, Eur. Phys. J. C **78**, 451 (2018).

[67] N. Gubernari, D. van Dyk, and J. Virto, Non-local matrix elements in $B_{(s)} \to \{K^{(*)}, \phi\}\ell^+\ell^-$, J. High Energy Phys. 02 (2021) 088.

[68] M. Beneke, T. Feldmann, and D. Seidel, Systematic approach to exclusive $B \to Vl^+l^-$, $V\gamma$ decays, Nucl. Phys. **B612**, 25 (2001).

[69] W. Altmannshofer, P. Ball, A. Bharucha, A. J. Buras, D. M. Straub, and M. Wick, Symmetries and asymmetries of $B \to K^*\mu^+\mu^-$ decays in the standard model and beyond, J. High Energy Phys. 01 (2009) 019.

[70] C. Bouchard, G. P. Lepage, C. Monahan, H. Na, and J. Shigemitsu, Rare decay $B \to K\ell^+\ell^-$ form factors from lattice QCD, Phys. Rev. D **88**, 054509 (2013); Erratum, Phys. Rev. D **88**, 079901 (2013).

[71] S. Descotes-Genon, L. Hofer, J. Matias, and J. Virto, Global analysis of $b \to s\ell\ell$ anomalies, J. High Energy Phys. 06 (2016) 092.

[72] B. Capdevila, S. Descotes-Genon, J. Matias, and J. Virto, Assessing lepton-flavour non-universality from $B \to K^*\ell\ell$ angular analyses, J. High Energy Phys. 10 (2016) 075.

[73] A. J. Buras, J. Girrbach-Noe, C. Niehoff, and D. M. Straub, $B \to K^{(*)}\nu\bar{\nu}$ decays in the Standard Model and beyond, J. High Energy Phys. 02 (**2015**) 184.

[74] A. K. Alok, B. Bhattacharya, D. Kumar, J. Kumar, D. London, and S. U. Sankar, New physics in $b \to s\mu^+\mu^-$: Distinguishing models through CP-violating effects, Phys. Rev. D **96**, 015034 (2017).

[75] A. K. Alok, B. Bhattacharya, A. Datta, D. Kumar, J. Kumar, and D. London, New physics in $b \to s\mu^+\mu^-$ after the measurement of R_{K^*}, Phys. Rev. D **96**, 095009 (2017).

[76] L. Calibbi, A. Crivellin, and T. Ota, Effective Field Theory Approach to $b \to s\ell\ell^{(\prime)}$, $B \to K^{(*)}\nu\bar{\nu}$ and $B \to D^{(*)}\tau\nu$ with Third Generation Couplings, Phys. Rev. Lett. **115**, 181801 (2015).

[77] R. Alonso, B. Grinstein, and J. Martin Camalich, Lepton universality violation and lepton flavor conservation in B-meson decays, J. High Energy Phys. 10 (2015) 184.

[78] G. Hiller and M. Schmaltz, R_K and future $b \to s\ell\ell$ physics beyond the standard model opportunities, Phys. Rev. D **90**, 054014 (2014).

[79] B. Gripaios, M. Nardecchia, and S. A. Renner, Composite leptoquarks and anomalies in B-meson decays, J. High Energy Phys. 05 (2015) 006.

[80] I. de Medeiros Varzielas and G. Hiller, Clues for flavor from rare lepton and quark decays, J. High Energy Phys. 06 (2015) 072.

[81] S. Sahoo and R. Mohanta, Scalar leptoquarks and the rare B meson decays, Phys. Rev. D **91**, 094019 (2015).

[82] S. Fajfer and N. Košnik, Vector leptoquark resolution of R_K and $R_{D^{(*)}}$ puzzles, Phys. Lett. B **755**, 270 (2016).

[83] D. Bečirević, S. Fajfer, and N. Košnik, Lepton flavor nonuniversality in $b \to s\ell^+\ell^-$ processes, Phys. Rev. D **92**, 014016 (2015).

[84] D. Bečirević, N. Košnik, O. Sumensari, and R. Zukanovich Funchal, Palatable leptoquark scenarios for lepton flavor violation in exclusive $b \to s\ell_1\ell_2$ modes, J. High Energy Phys. 11 (2016) 035.

[85] A. Greljo, G. Isidori, and D. Marzocca, On the breaking of lepton flavor universality in B decays, J. High Energy Phys. 07 (2015) 142.

[86] C.-W. Chiang, X.-G. He, and G. Valencia, Z' model for $b \to s\ell$ flavor anomalies, Phys. Rev. D **93**, 074003 (2016).

[87] R. Gauld, F. Goertz, and U. Haisch, On minimal Z' explanations of the $B \to K^*\mu^+\mu^-$ anomaly, Phys. Rev. D **89**, 015005 (2014).

[88] R. Gauld, F. Goertz, and U. Haisch, An explicit Z'-boson explanation of the $B \to K^*\mu^+\mu^-$ anomaly, J. High Energy Phys. 01 (2014) 069.

[89] A. Crivellin, L. Hofer, J. Matias, U. Nierste, S. Pokorski, and J. Rosiek, Lepton-flavour violating B decays in generic Z' models, Phys. Rev. D **92**, 054013 (2015).

[90] I. Ahmed and A. Rehman, LHCb anomaly in $B \to K^*\mu^+\mu^-$ optimised observables and potential of Z' Model, Chin. Phys. C **42**, 063103 (2018).

[91] W. Buchmuller, R. Ruckl, and D. Wyler, Leptoquarks in lepton—quark collisions, Phys. Lett. B **191**, 442 (1987); Erratum, Phys. Lett. B **448**, 320 (1999).

[92] P. Langacker and M. Plumacher, Flavor changing effects in theories with a heavy Z' boson with family nonuniversal couplings, Phys. Rev. D **62**, 013006 (2000).

[93] V. Barger, C.-W. Chiang, P. Langacker, and H.-S. Lee, Z' mediated flavor changing neutral currents in B meson decays, Phys. Lett. B **580**, 186 (2004).

[94] V. Barger, C.-W. Chiang, P. Langacker, and H.-S. Lee, Solution to the $B \to \pi K$ puzzle in a flavor-changing Z-prime model, Phys. Lett. B **598**, 218 (2004).

[95] P. A. Zyla *et al.*, Review of particle physics, Prog. Theor. Exp. Phys. **2020**, 083C01 (2020).

[96] C. B. Lang, D. Mohler, S. Prelovsek, and R. M. Woloshyn, Predicting positive parity B_s mesons from lattice QCD, Phys. Lett. B **750**, 17 (2015).

[97] C. Bourrely, I. Caprini, and L. Lellouch, Model-independent description of $B \to \pi l\nu$ decays and a determination of $|V_{ub}|$, Phys. Rev. D **79**, 013008 (2009); Erratum, Phys. Rev. D **82**, 099902 (2010).